GENERALIZED PAGING SCHEMES FOR CELLULAR SYSTEMS

by

TAE KYUNG KIM

B.A.Sc. (E.E.), University of British Columbia, 1995

A THESIS SUBMITTED IN PARTIAL FULFILLMENT OF

THE REQUIREMENTS FOR THE DEGREE OF

MASTER OF APPLIED SCIENCE

in

THE FACULTY OF GRADUATE STUDIES

DEPARTMENT OF ELECTRICAL AND COMPUTER ENGINEERING

We accept this thesis as conforming to the required standard

THE UNIVERSITY OF BRITISH COLUMBIA

May 1998

© Tae Kyung Kim, 1998

Department of _Electrical and Computer Engineering_

The University of British Columbia
Vancouver, Canada

Date _May 27, 1998_

DE-6 (2/88)

Abstract

The problem of locating a mobile vehicular user in a cellular communication system is addressed. Two location area (LA) paging schemes, called *generalized paging with time-stamp* and *generalized paging without time-stamp*, are proposed to determine the location of a user within an LA and are compared to the *Selective paging* scheme. The mobility of a user is modelled by a directional random walk process and the user location is registered using a dynamic LA-based location updating scheme. It is found that *generalized paging with time-stamp* and *generalized paging without time-stamp* can significantly reduce both average paging delay and traffic when compared to *Selective paging*.

The sensitivity of the two generalized paging schemes to uncertainty in user mobility parameter values, such as the mean speed, mean velocity hold time, and angular deviation parameter, is studied. *Generalized paging with time-stamp* is found to be very sensitive to uncertainty in user mean speed whereas *generalized paging without time-stamp* is not very sensitive to changes in all three parameter values.

Two multicasting schemes called *generalized multicasting with time-stamp* and *generalized multicasting without time-stamp*, based on the two *generalized paging* schemes, are proposed. The two *generalized multicasting* schemes' performances in terms of the average paging delay and traffic improve significantly as the number of users within the service area is increased.

Table of Contents

List of Figures

Acknowledgment

I would like to express my sincerest gratitude to my research supervisor, Dr. Cyril Leung, for his invaluable advice and constant guidance during the course of my research.

I also thank my friends and colleagues at the University of British Columbia who made my studies here more enjoyable and rewarding. Especially, I would like to thank Byung-Kyu Chun, Sinclair Chi, Chris Kim, Peter Kim, and Andrew Chung for their valuable friendship and encouragements. They always bring smiles to my face.

Finally, but foremost, I would like to thank my family for their endless love. I dedicate my hard work to my parents who are watching me from above.

Chapter 1 INTRODUCTION

Conventional personal communication technologies, such as telephones, can no longer fully satisfy the needs of today's highly mobile people. Now there is a growing demand for a communication system that enables its subscribers to initiate and receive calls without any restrictions on their locations. To provide such a capability, cellular communication networks were introduced in the early 1980's. Since its introduction, cellular communication systems around the world have been enjoying 33 percent to 50 percent growth rates [1]. Cellular communication is evolving from a costly service with limited availability toward an affordable alternative to the wired telephone service [2].

1.1 Background

The major drawback of a conventional wireless communication system that uses one base station with a powerful multi-channel radio transceiver is the limited wireless bandwidth. To support a large number of subscribers with a limited number of wireless channels, a "cellular" architecture was developed. Instead of having one high power base station, a cellular network employs a number of low power base stations, each covering a small surrounding area called a "cell". The service area is partitioned into cells, and each cell is assigned a number of channels. Although the number of active connections within each cell cannot exceed the number of channels available, the same channels may be reused in another cell as long as the two cells are separated by a sufficiently large distance to limit the interference [1]. By using the same channel in more than one cell, the cellular network is able to support more subscribers.

In order to deliver incoming calls to the mobile terminals (MT's) roaming in the service area, the mobile switching center (MSC) needs to keep track of each MT's location. This is

referred to as mobility management. A number of cells are grouped to form a location area (LA), and each MT reports its current LA to the system according to the location updating scheme. The location updating scheme determines when and how often the MT's location should be registered with the MSC. When a call comes in for a subscriber, the MSC delivers the call to the MT by paging the MT's last known LA. The paging process follows the paging scheme. Efficient location updating and paging schemes are needed to reduce the paging delay and traffic. Many location updating schemes have been studied in [1], [3], [4], [5], and [6]. Also, various paging schemes have been proposed in [3], [7], [8], [9], and [10].

1.2 Motivations and Objectives

When a call comes in for a mobile user, the cells in the user's last registered LA are paged. The most commonly used paging scheme, *Flood paging*, requires sending a paging signal to all the cells in the LA. In order to support the rapidly increasing number of subscribers, a cellular network needs a more efficient paging scheme. If a mobility model for MT's is available, the probability of an MT being in a given cell in the LA can be estimated. Then, cells in the LA can be grouped into subsets and each subset can be paged successively until the MT is found. The paging delay will be higher than when using *Flood paging*. However, by carefully grouping cells, the increase in the average paging delay can be kept small while greatly reducing the average paging traffic.

The main objectives of this thesis are:

1. To study the groupings of cells in the LA for successive paging stages.

2. To study the trade-off between the average paging delay and the paging traffic.

3. To study the effects of making use of elapsed time since the last location update.

4. To study the effects of uncertainty in choosing user mobility model parameters.

5. To implement multicasting schemes using paging schemes

1.3 Outline of the Thesis

In Chapter 2, a mobility model for a mobile vehicular user is described. In Chapter 3, a location updating scheme is described along with the cell and LA geometries. In Chapter 4, two different *generalized paging* schemes are proposed. The first generalized paging scheme will use the elapsed time since the last location update to estimate the mobile user's current location. The second *generalized paging* scheme will try to locate a mobile user without using the elapsed time since the last location update. The two schemes' average paging delays and average paging traffics are evaluated by both simulation and approximation. The results are compared to *Selective paging*. We evaluate the gain in performance when the time elapsed since last location update is used to make paging decisions. In Chapter 5, the sensitivity of the *generalized paging* schemes to uncertainty in user mobility parameter values is studied. *Generalized paging* schemes are used to implement *generalized multicasting* schemes in Chapter 6. The main results are summarized in Chapter 7 and some suggestions for future work are listed.

Chapter 2 USER MOBILITY MODEL

In order to describe mobile users' movements within the service area, a reasonable mobility model is needed. Different mobility models, such as the uniformly distributed model described in [3], have been proposed previously. However, considering the layouts of roads and the fact that a mobile telephone user tends to travel toward a certain destination, a directional random walk [11] seems to be a better mobility model. In Chapter 3 and Chapter 4, it will be used as the mobility model of a vehicular telephone user.

2.1 Review of Directional Random Walk Model of [11]

In the directional random walk model, a mobile user is assumed to travel toward the principal direction in discrete and statistically independent steps, where the principal direction is defined by the path drawn from each movement step's starting point to the destination. For each movement step, the user selects a random angular deviation β with p.d.f. $f_B(\beta)$ from the principal direction, a random speed v with p.d.f. $f_V(v)$, and a random holding time t_h with p.d.f. $f_h(t)$; thus for the duration t_h of this step, the user maintains the chosen angular deviation and speed. This random walk model is illustrated in Figure 2.1.
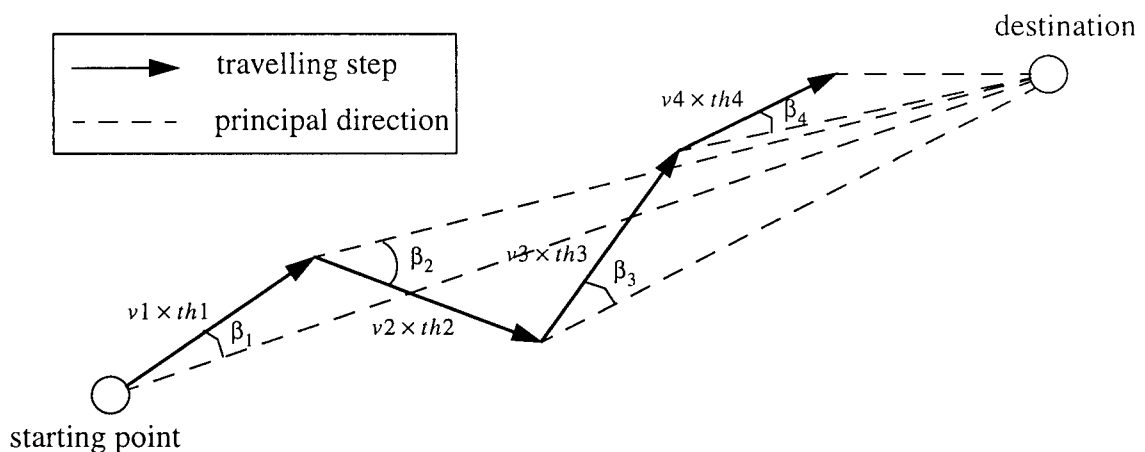
Figure 2.1 Random walk model

The speed distribution is assumed to be Gaussian with standard deviations of 0.17 times the respective means. Thus,

$$f_V(v) = \frac{1}{\sqrt{2\pi\sigma_d^2}} e^{\frac{-(v - \bar{v})^2}{2\sigma_d^2}} \tag{2.1}$$

where $\sigma_d = 0.17 \times \bar{v}$.

To describe the distribution of mobile users' angular deviations from the principal directions, an Alpha p.d.f. is used with mean deviation of zero.

$$f_B(\beta) = \begin{cases} \dfrac{1}{2} \dfrac{\alpha_\beta}{\left[1 + \alpha_\beta^2\beta^2\right]\tan^{-1}(\alpha_\beta\pi)} & ; \quad -\pi \le \beta \le \pi \\ \\ 0 & ; \quad otherwise \end{cases} \tag{2.2}$$

Assuming that a mobile user moves in the forward direction with a probability of 0.95, the parameter, α_β, is set to 4.2. The p.d.f. is plotted in Figure 2.2.

The p.d.f. of the holding time for each step, $f_h(t)$, is modeled by an exponential distribution with parameter $\lambda_h = \dfrac{1}{\bar{t}_h}$ where $\bar{t}_h$ is the mean holding time, i.e.

$$f_h = \begin{cases} \lambda_h e^{-\lambda_h t} & ; \quad t \ge 0 \\ 0 & ; \quad otherwise \end{cases} \tag{2.3}$$
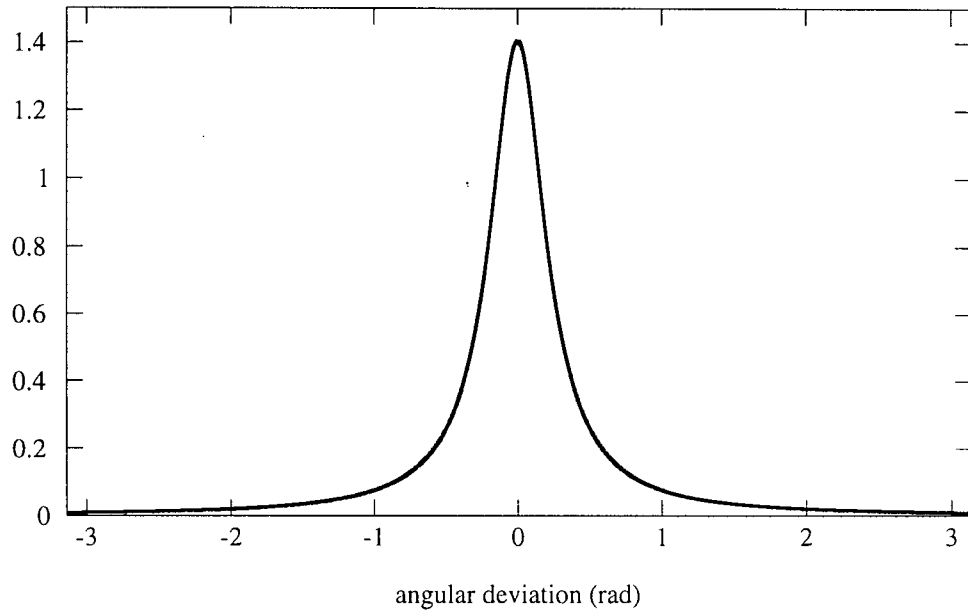
Figure 2.2 Angular deviation p.d.f. with $\alpha_\beta = 4.2$

2.2 Simulation results

Using the directional random walk mobility model, the p.d.f of the radial distance from the starting point given the travel time t, $f_R(r|t)$, is obtained through simulation. Also, the p.d.f of the angular deviation from the principal direction given the travel time t, $f_\Theta(\theta|t)$, is obtained. The destination is assumed to be at infinite distance from the starting point for the random walk simulation. The required parameters for the random walk model simulation are the mean speed, $\bar{v}$, and mean holding time, $\overline{t_h}$. The simulations are based on the time increments of 4 seconds and the sample size is 400,000 trips for each p.d.f. The frequency distributions of the radial distance and angular deviation are obtained with sampling bin sizes of 175 m and 0.01π respectively. Then the frequency distributions of the radial distance and angular deviation are normalized by the number of samples and are scaled by $\frac{1}{\Delta r}$ and $\frac{1}{\Delta\theta}$ to estimate the radial distance and angular deviation p.d.f.'s. The radial distance and angular deviation p.d.f.'s obtained from simulation are

shown in Figure 2.3 and Figure 2.4. The 99% confidence interval associated with each simulation point is within ±5 % of the average values plotted throughout this thesis.

2.3 Approximating the Radial Distance and Angular Deviation P.d.f.'s

It is very hard to derive the analytical expressions of the radial distance p.d.f. $f_R(r|t)$ and the angular deviation p.d.f. $f_\Theta(\theta|t)$ from the random walk model. Thus, $f_R(r|t)$ and $f_\Theta(\theta|t)$ obtained from simulations (in Section 2.2) are used to approximate their analytical forms.

2.3.1 Radial distance p.d.f.

For convenience, the starting point is assumed to be at the origin of a Cartesian coordinate system and the destination is assumed to be at $+\infty$ on the x-axis. The units for time, distance, and speed are in seconds, meters, and meters per second respectively.

The radial distance p.d.f. $f_R(r|t)$ obtained from simulation is fitted by an asymmetric Gaussian p.d.f., i. e.

$$f_R(r|t) \approx \begin{cases} A_1 \dfrac{1}{\sqrt{2\pi\sigma_1^2}} e^{-\dfrac{(r-m)^2}{2\sigma_1^2}} & ; \quad r < m \\[4mm] A_2 \dfrac{1}{\sqrt{2\pi\sigma_2^2}} e^{-\dfrac{(r-m)^2}{2\sigma_2^2}} & ; \quad m \le r \end{cases} \tag{2.4}$$

where $\sigma_2 = \gamma\sigma_1$, $A_1 = \dfrac{2}{1+\gamma}$, and $A_2 = \dfrac{2\gamma}{1+\gamma}$.

In order to obtain an approximate expression for $f_R(r|t)$ at time t, the three parameters of the asymmetric Gaussian p.d.f., σ_1, γ, and m, must be obtained as functions of time.
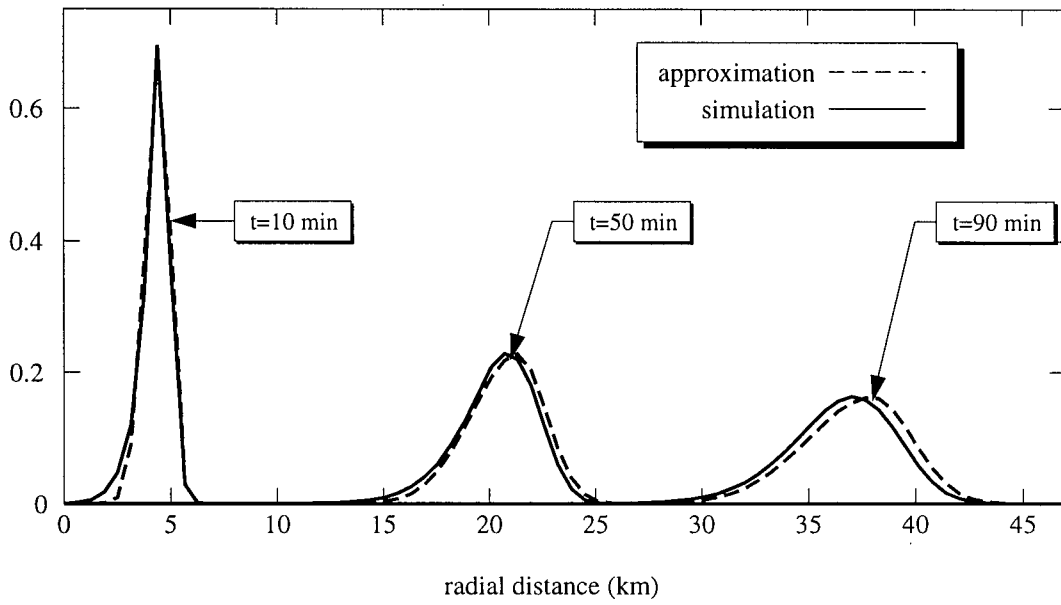
Figure 2.3 Radial distance p.d.f. of random walk from simulation with $\bar{v} = 30$ km/hr and $\overline{t_h} = 60$ sec.
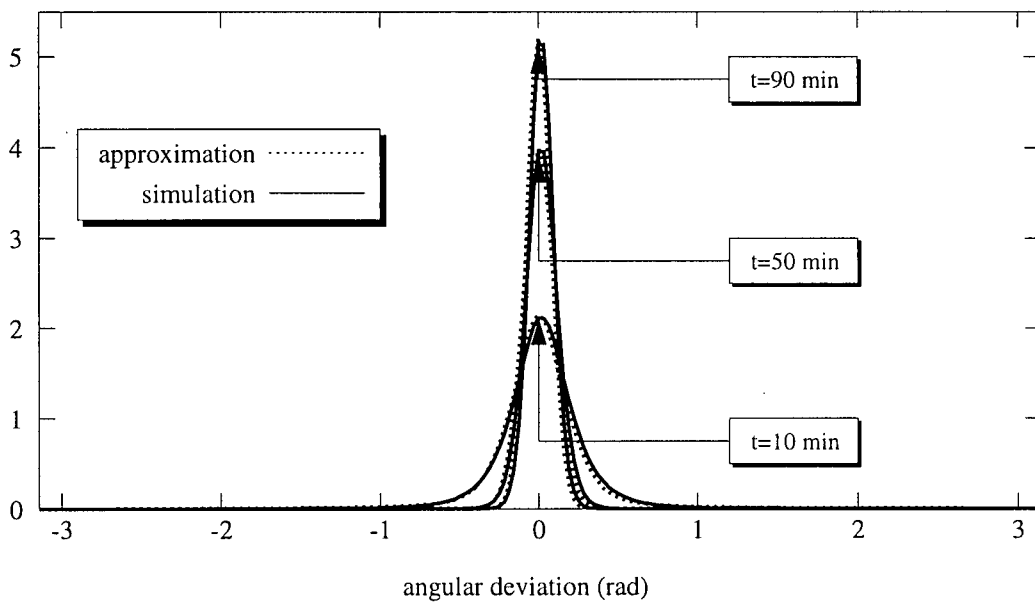
Figure 2.4 Angular deviation p.d.f. from simulation with $\bar{v} = 30$ km/hr and $\overline{t_h} = 60$ sec.

From [11],

$$\sigma_1^2 = \left\{ \frac{A_1}{max[f_R(r|t)]} \right\}^2 \frac{1}{2\pi} \tag{2.5}$$

and

$$max[f_R(r|t)] \approx max[f_X(x|t)] \tag{2.6}$$

As shown in Figure 2.5, the x-displacement D_x of the mobile user after time t can be expressed as the sum of the x-components of the travelling steps taken, i.e.,

$$D_x \approx \sum_{i=1}^{N(t)} x_i \tag{2.7}$$

where $x_i = v_i t_{h_i} \cos(\beta_i)$ and $N(t)$ = number of steps taken in time t.

In [11], it is assumed that D_x has a Gaussian distribution by nature of the central limit theorem. However, based on the simulation results, it is found that this assumption is not very accurate. In
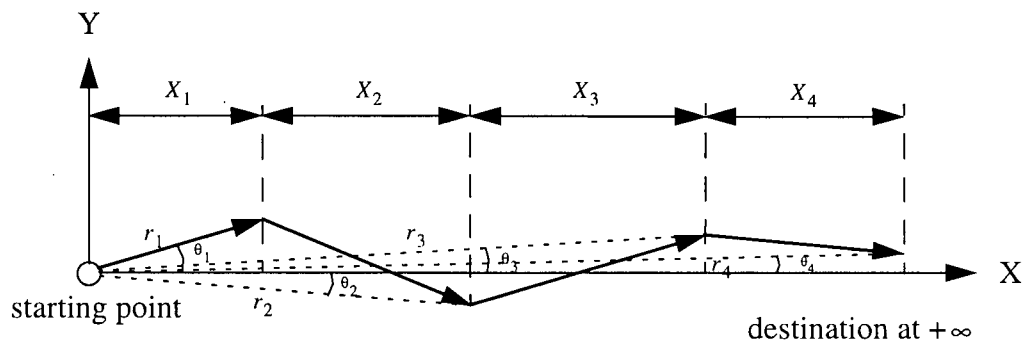
Figure 2.5 Analytical directional random walk model

order to more accurately approximate $f_X(x|t)$, a multiplicative correction function $f_a(t)$ is applied to the Gaussian distribution. The peak value of $f_X(x|t)$ is then

$$max[f_X(x|t)] = \frac{f_a(t)}{\sqrt{2\pi\sigma_{D_x}^2}} \qquad (2.8)$$

Since each travelling step is statistically independent and D_x has the property shown in Eqn. (2.7),

$$\sigma_{D_x}^2 \approx N(t)\sigma_x^2. \qquad (2.9)$$

where

$$\begin{aligned}
\sigma_x^2 &= \overline{x^2} - (\bar{x})^2 \\
&= \overline{v^2 t_h^2 \cos^2(\beta)} - \left(\overline{v t_h \cos(\beta)}\right)^2 \\
&= \overline{v^2}\,\overline{t_h^2}\,\overline{\cos^2(\beta)} - \left(\bar{v}\,\overline{t_h}\,\overline{\cos(\beta)}\right)^2
\end{aligned} \qquad (2.10)$$

$\sigma_{D_x}^2$ can be obtained numerically, and the required adjusting function $f_a(t)$ is found to be

$$f_a(t) = -1.87 \times 10^{-11} t^3 + 2.2 \times 10^{-7} t^2 - 8.658 \times 10^{-4} t + 3.0636 \qquad (2.11)$$

Note that, since t can range from 0 to 5400 seconds, the cubic term is not necessarily negligible.

From Eqn. (2.6), Eqn. (2.8), and Eqn. (2.9), we have

$$max[f_R(r|t)] \approx max[f_X(x|t)]$$

$$= \frac{f_a(t)}{\sqrt{2\pi N(t)\sigma_x^2}} \tag{2.12}$$

In [11], $N(t)$ is obtained by solving Eqn. (2.12) (without $f_a(t)$) for $N(t)$ using the values of $max[f_R(r|t)]$ from simulation. However, the values of $N(t)$ found in [11] do not seem to represent the number of steps taken by the mobile user in time t, which should have the expected value of $\frac{t}{\overline{t_h}}$. A more direct method is applied to obtain $N(t)$ instead. Since $N(t)$ is the number of steps travelled in time t, $N(t)$ is obtained from simulation by counting the number of steps taken by the mobile user at time t. Five different parameter sets are used to plot Figure 2.6, and the five different curves show the same relationship. After curve fitting,

$$N(t, \overline{t_h}) = -6.94 \times 10^{-8}\left(\frac{t}{\overline{t_h}}\right)^3 + 1.85 \times 10^{-5}\left(\frac{t}{\overline{t_h}}\right)^2 + 9.350 \times 10^{-1}\left(\frac{t}{\overline{t_h}}\right) + 0.2134 \tag{2.13}$$

By substituting Eqn. (2.12) into it, Eqn. (2.5) can now be expressed as

$$\sigma_1^2 \approx \frac{A_1^2 N(t, \overline{t_h})\sigma_x^2}{f_a(t)} \tag{2.14}$$

Next, the parameter γ, which represents the ratio between the variances of the first half Gaussian p.d.f. and the second half Gaussian p.d.f. in the asymmetric Gaussian p.d.f., is approximated by

$$\gamma(\overline{t_h}) = -1.21 \times 10^{-7}(\overline{t_h})^3 + 5.224 \times 10^{-5}(\overline{t_h})^2 - 7.159 \times 10^{-3}(\overline{t_h}) + 0.8813 \tag{2.15}$$

Finally, by rearranging Eqn. (B.10), the parameter m can be expressed as

$$m(t, \overline{t_h}) = \overline{r(\overline{v}, t, \overline{t_h})} - \sqrt{\frac{2}{\pi}}\sigma_1[\gamma(\overline{t_h}) - 1] \tag{2.16}$$
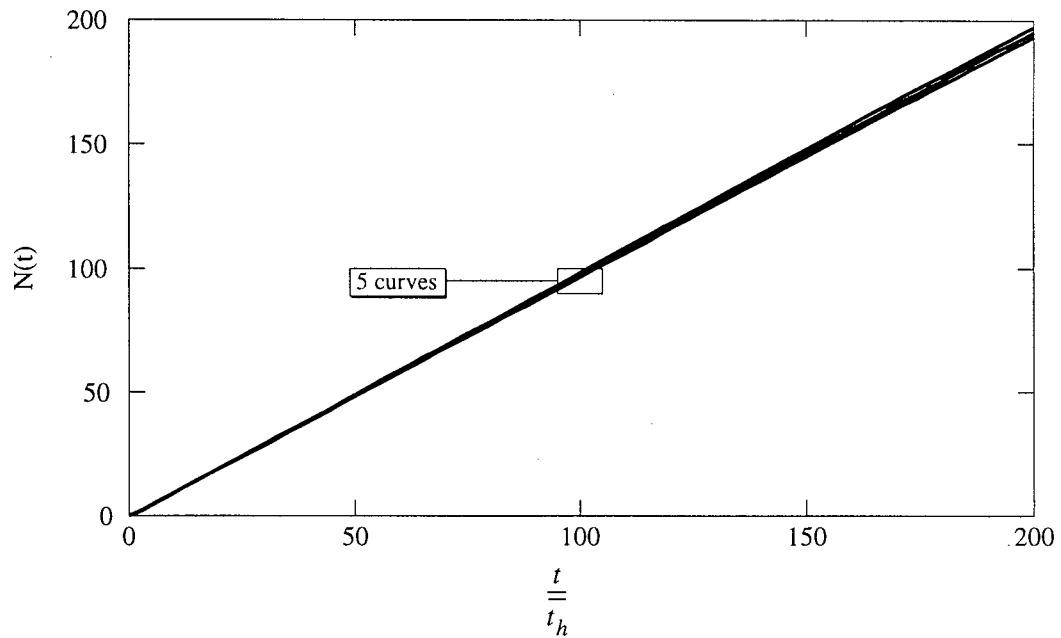
Figure 2.6 Plot of N(t) versus $\frac{t}{\bar{t}_h}$ for parameter sets $\{\bar{v}$ km/hr, $\bar{t}_h$ sec$\}$: $\{20, 30\}$, $\{30, 60\}$, $\{30, 180\}$, $\{40, 30\}$, and $\{50, 90\}$

where $r(\bar{v}, t, \bar{t}_h)$ is the mean radial distance of the mobile user at time t with the mean holding

time $\bar{t}_h$ and can be approximated by adding an offset value to the mean distance in x direction as

$$\overline{r(\bar{v}, t, \bar{t}_h)} = \overline{x(t, \bar{v}, \beta)} + c(\bar{v}, \bar{t}_h)$$
$$= \overline{\bar{v}\cos(\beta)}t + c(\bar{v}, \bar{t}_h) \tag{2.17}$$

The offset $c(\bar{v}, \bar{t}_h)$ is approximated as

$$c(\bar{v}, \bar{t}_h) = 3.24(\bar{v})^2 - 37.8(\bar{v}) + 0.0096(\bar{t}_h)^2 + 1.3586(\bar{t}_h) + 150.3608 \tag{2.18}$$

The resulting approximate radial distance p.d.f.'s are plotted in Figure 2.3. The goodness

of fit of the radial distance p.d.f. is obtained by integrating the absolute difference between the

approximate and simulation pd.f.'s. Figure 2.7 shows the goodness of fit for various random walk

parameter sets.
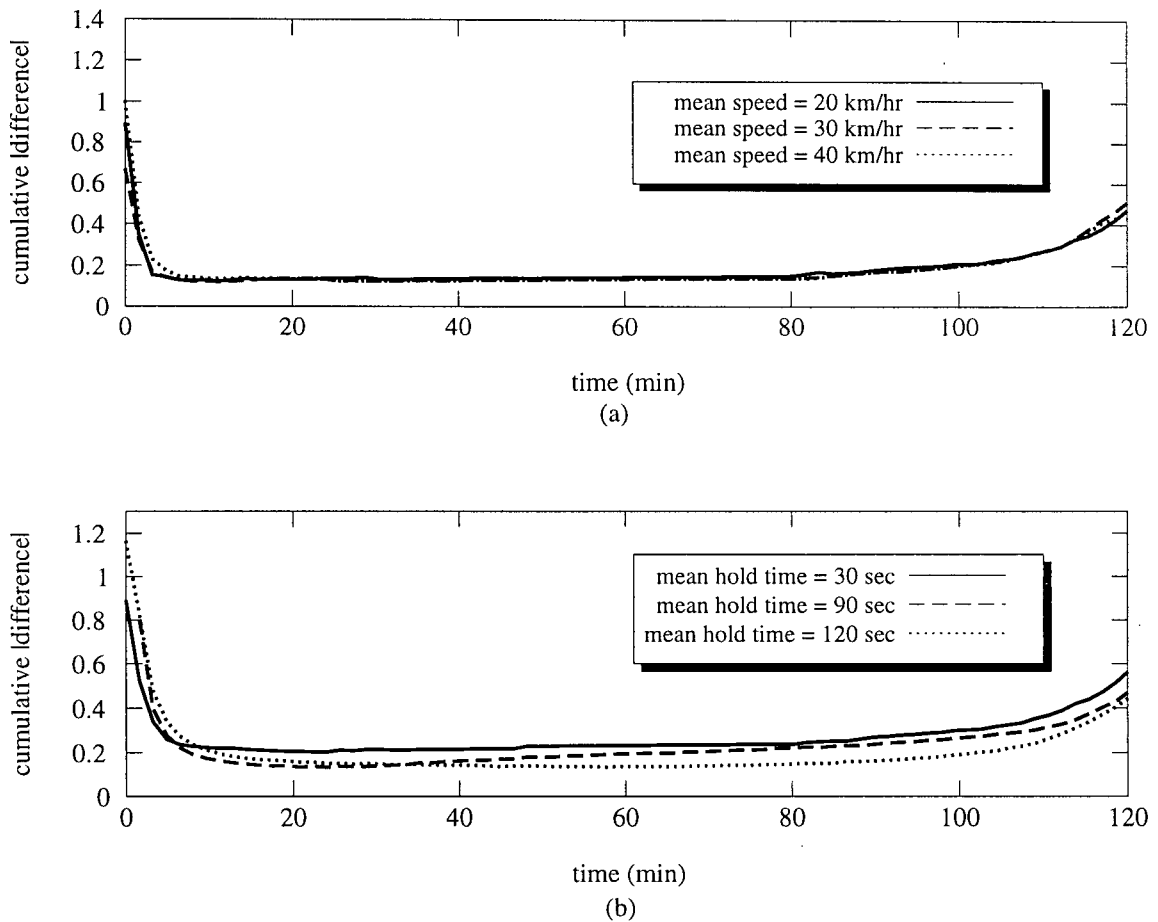
Figure 2.7 Goodness of fit of the approximate radial distance p.d.f. (a) $\bar{t}_h$ = 60 sec (b) $\bar{v}$ = 50 km/hr

The goodness of fit is shown in terms of the cumulative difference. The cumulative difference represents the non-overlapping area between two p.d.f.'s. Thus the maximum cumulative difference value is 2 (no overlapping occurs) and the minimum cumulative difference value is 0 (two p.d.f.'s are identical).

2.3.2 Angular deviation p.d.f.

The angular deviation p.d.f. is fitted by a Gaussian p.d.f. when t is small and by an Alpha p.d.f. when t is large. Thus, the angular deviation p.d.f., $f_\Theta(\theta|t)$, is approximated by combining these two p.d.f.'s with a weighting function of t, and can be expressed as

$$f_\Theta(\theta|t) \approx \rho(t)f_G(\theta|t) + [1 - \rho(t)]f_A(\theta|t) \tag{2.19}$$

where $f_G(\theta|t)$ is the Gaussian p.d.f., $f_A(\theta|t)$ is the Alpha p.d.f., and $\rho(t)$ is the weighting function which produces a positive number less than or equal to 1.

The Gaussian p.d.f., $f_G(\theta|t)$, is expressed as

$$f_\Theta(\theta|t) = \frac{1}{\sqrt{2\pi\sigma_2^2(t)}} e^{-\frac{\theta^2}{2\sigma_G^2(t)}} \tag{2.20}$$

where $\sigma_G^2(t)$, the variance estimated by noting the peak values of p.d.f.'s from simulation, is

$$\sigma_G^2(t, \overline{t_h}) = \begin{cases} \begin{aligned} &1.8613 \times 10^{-7}\left(\frac{t}{t_h}\right)^4 - 1.5580 \times 10^{-5}\left(\frac{t}{t_h}\right)^3 \\ &+ 5.0597 \times 10^{-4}\left(\frac{t}{t_h}\right)^2 - 0.0083\left(\frac{t}{t_h}\right) \\ &+ 0.0805 \end{aligned} & ; \quad 0 \le \left(\frac{t}{t_h}\right) \le 27 \\[2em] 0.08e^{-0.3344\left(\frac{t}{t_h}\right)^{\frac{1}{2}}} + 0.0025 & ; \quad 27 \le \left(\frac{t}{t_h}\right) \le 132 \\[2em] 0.08e^{-0.3\left(\frac{t}{t_h}\right)^{\frac{1}{2}}} + 0.0017 & ; \quad 132 \le \left(\frac{t}{t_h}\right) \end{cases} \tag{2.21}$$

The Alpha p.d.f., $f_A(\theta|t)$, is expressed as

$$f_A(\theta|t) = \begin{cases} \dfrac{1}{2}\dfrac{\alpha_A(t)}{\left[1 + \alpha_A^2(t)\theta^2\right]\tan^{-1}(\alpha_A(t)\pi)} & ; \quad -\pi \le \theta \le \pi \\[1em] 0 & ; \quad otherwise \end{cases} \tag{2.22}$$

$\alpha_A(t)$ is approximated to be

$$\alpha_A(t, \overline{t_h}) = \frac{1}{\varpi(t, \overline{t_h})}$$ (2.23)

where

$$\varpi(t, \overline{t_h}) = \begin{cases} \begin{aligned} &-5.9969 \times 10^{-6}\left(\frac{t}{\overline{t_h}}\right)^3 + 4.1880 \times 10^{-4}\left(\frac{t}{\overline{t_h}}\right)^2 \\ &- 0.0117\left(\frac{t}{\overline{t_h}}\right) + 0.2335 \end{aligned} & ; \quad 0 \le \left(\frac{t}{\overline{t_h}}\right) \le 25 \\[2em] \begin{aligned} &-2.7376 \times 10^{-7}\left(\frac{t}{\overline{t_h}}\right)^3 + 4.9513 \times 10^{-5}\left(\frac{t}{\overline{t_h}}\right)^2 \\ &- 0.0036\left(\frac{t}{\overline{t_h}}\right) + 0.1718 \end{aligned} & ; \quad 25 \le \left(\frac{t}{\overline{t_h}}\right) \le 60 \\[2em] 0.0840e^{-\frac{1}{65}\left(\frac{t}{\overline{t_h}}\right)} + 0.0412 & ; \quad 60 \le \left(\frac{t}{\overline{t_h}}\right) \le 120 \\[2em] 0.0600e^{-\frac{1}{122}\left(\frac{t}{\overline{t_h}}\right)} + 0.0319 & ; \quad 120 \le \left(\frac{t}{\overline{t_h}}\right) \end{cases}$$ (2.24)

As the weighting function, $\rho(t)$, a scaled and vertically shifted arctan function is used to provide a smooth transition from 0 to 1.

$$\rho(t, \overline{t_h}) = \frac{1}{\pi}\tan^{-1}\left[a\left(\frac{t}{\overline{t_h}}\right) - b\right] + \frac{1}{2}$$ (2.25)

The parameters a and b, which control the function's rate of change, are set to be 0.1 and 1 respectively. The goodness of fit of the angular deviation p.d.f. is obtained by integrating the absolute difference between the approximate and simulation p.d.f.'s. Figure 2.8 shows the goodness of fit for various random walk parameter sets.

(a)

(b)
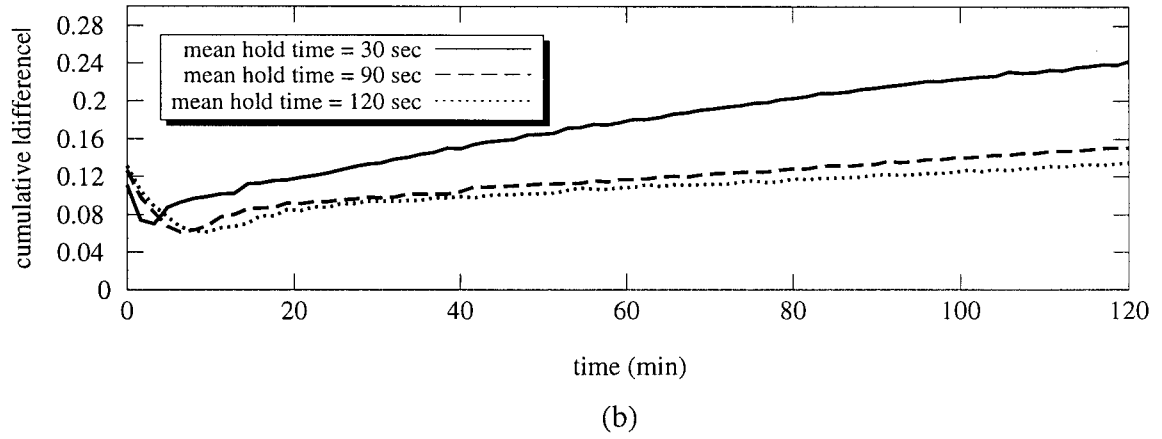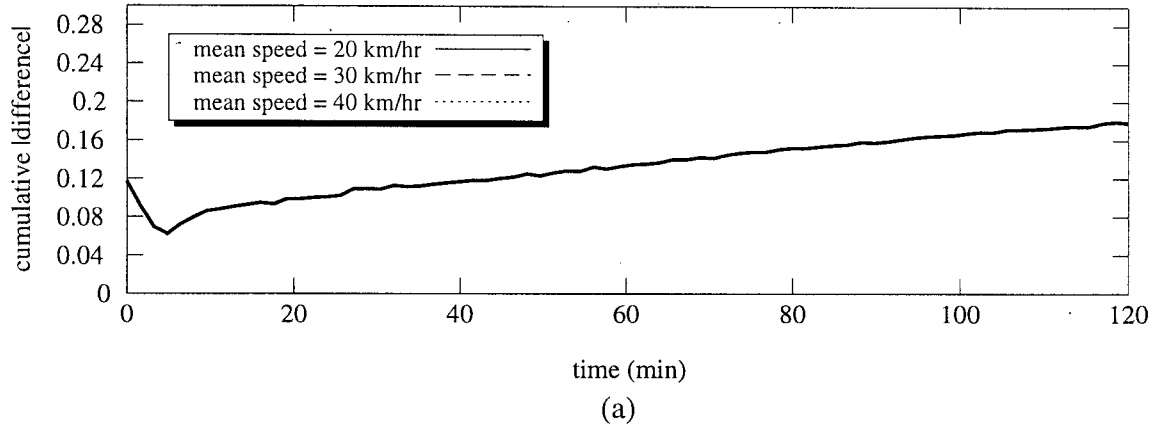
Figure 2.8 Goodness of fit of the analytical angular deviation p.d.f. (a) $\overline{t_h}$ = 60 sec (b) $\overline{v}$ =50 km/hr

Chapter 3 CELLULAR LAYOUT AND LOCATION AREA
UPDATING SCHEME

In this chapter, the layout of cells and the structure of a location area in a cellular environment are described along with the dynamic LA-based location updating scheme, which will be used throughout this thesis.

3.1 Cellular Layout Model

The service area of a cellular communications network is divided into smaller units, called *cells*. All cells are assumed to have the same size and shape. As shown in Figure 3.1, cells are usually assumed to be hexagonal in shape. Each cell has a base station (BS) in it for its coverage. The BS in a cell broadcasts a unique identity number and the mobile users can listen in while they are within the cell's coverage area. A mobile user can identify the cell he is in by choosing the BS from which the strongest signal is received.
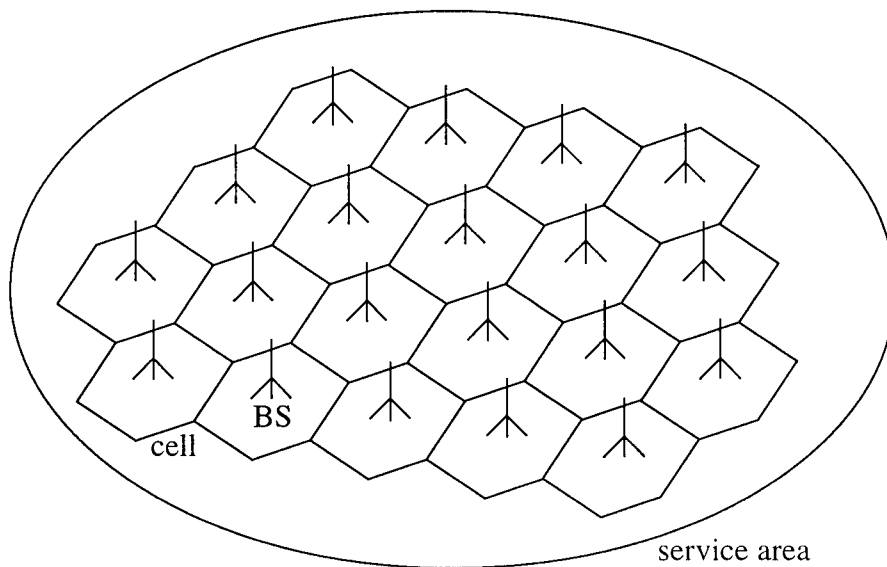
Figure 3.1 Cellular System Layout Model

3.2 Location Area

Current cellular networks partition their service areas into a number of location areas (LA's). Each LA consists of a group of cells and each mobile user performs a location update whenever it crosses an LA boundary [12]. Thus a mobile user's current LA is always known.

Each LA has a number of rings of cells. The innermost ring (ring 0) consists of only one cell and this is the center cell. Ring 0 is surrounded by ring 1 which in turn is surrounded by ring 2, and so on. The size of an LA is determined by the number of rings the LA has. Figure 3.2 shows an LA of size 4.
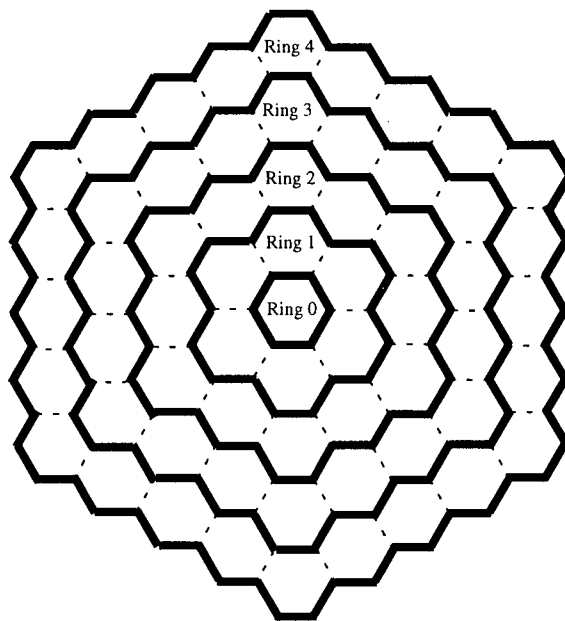
Figure 3.2 Location Area of size = 4

For simulation, hexagonal cell shapes are assumed. However, for the purpose of mathematical analysis, the rings in an LA are taken to be circular. The equivalent radius, r_{eqv}, of a cell is the radius of a circle that has the same area as a hexagonal cell as shown in Figure 3.3.
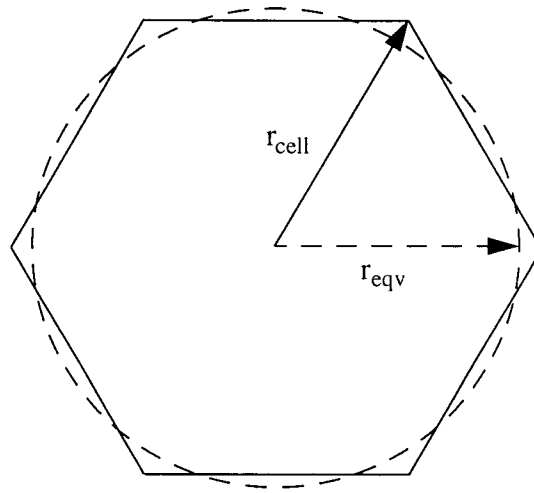
Figure 3.3 Equivalent radius of a cell

$$\pi r_{eqv}^2 = 6\left[\frac{1}{2}r_{cell}^2\sin\left(\frac{\pi}{3}\right)\right] \tag{3.1}$$

or

$$r_{eqv} = r_{cell}\sqrt{\frac{3}{\pi}\sin\left(\frac{\pi}{3}\right)} \tag{3.2}$$

$$= 0.9094\,r_{cell}$$

For an LA, the rings are considered to be circular also. For the kth ring, the equivalent radius, $R_{eqv}(k)$, is the radius of a circle that has the same area as the total area of all cells in rings, 1, 2, ..., k. From [11],

$$R_{eqv}(k) = r_{eqv}\sqrt{N(k)} \tag{3.3}$$

where $N(k)$ is the total number of cells in rings 1, 2, 3, ..., k.

$$N(k) = 1 + 3k(1 + k) \tag{3.4}$$
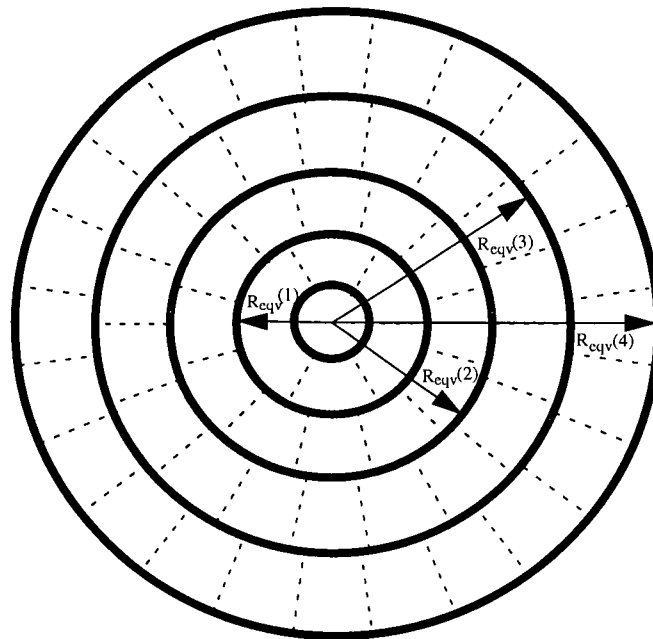
Figure 3.4 Circular LA model of size = 4

3.3 Location Updating Scheme

According to the location updating scheme, each mobile user registers its current location with the system. Thus different location updating schemes will result in different location updating traffic in a cellular system. Since the control channel capacity is limited by the location updating and paging signal traffic, an effective location updating scheme is very important. Generally, location updating schemes can be divided into two groups: static and dynamic. In static LA-based scheme, location updates are performed when mobile users cross fixed LA boundaries. Although they are simple to implement, static LA-based schemes are not very efficient since a mobile user travelling near LA boundaries will generate an excessive amount of location updating traffic. Dynamic LA-based schemes allow a new LA to be formed each time a mobile user crosses an LA boundary so that the mobile user is placed at the center of the new LA. In [5], a dynamic location updating scheme using overlapping LA's is proposed. When a mobile user updates his

location to the system, the cell he is currently in is reported as the center cell of the new LA. Having received the update from the mobile user, the system determines the new LA's member cells and sends their i.d.'s to the mobile user. The user can now use these i.d.'s to determine if he has exited the LA by comparing them to the i.d.'s broadcast by the current cell. Throughout this thesis, it will be used as the location updating scheme.

3.3.1 Location updating conditions

A location update is performed when any of the following 4 events occurs.

1. *The mobile user starts a journey.*

The initial location update at the start defines the first LA and lets the system know the user is ready to move.

2. *The mobile user crosses an LA boundary.*

When a mobile user exits the LA, a location update is performed to determine a new LA.

3. *A call comes in for the mobile user.*

When a call comes in for the mobile user, a location update is performed during the call setup. The current location of the mobile user in the LA can be obtained without having an additional connection to the system.

4. *The mobile user ends a journey.*

A final location update is performed when the mobile user reaches the destination. It notifies the system that the user will be in the current location until event 1 occurs.

3.3.2 Location updating traffic

We define a location updating traffic as a registration of the mobile user's location with the system. The location updating traffic resulting from event 1 (the mobile user starts a journey), event 2 (the mobile user crosses a LA boundary), and event 4 (the mobile user ends a journey) is obtained by simulation and approximation. Since the location update due to the event 3 (a call comes in for the mobile user) is performed during the call setup, it is not considered here.

To approximate the location updating traffic due to the event 2, the time a mobile user takes to exit an LA, t_{cross}, is estimated by

$$t_{cross} \approx R_{eqv}(R) \times \frac{1}{\bar{v}_p} \tag{3.5}$$

where R is the size of the LA in number of rings and $\bar{v}_p$ is the mobile user's speed in the principal direction. The user's speed in the principal direction is

$$\bar{v}_p = \bar{v} \cdot \overline{\cos(\phi)} \tag{3.6}$$

where $\bar{v}$ is the mobile user's mean speed and ϕ is the angular deviation of the user's travelling direction from the principal direction. Then the location updating traffic per unit time resulting from LA boundary crossings, $\overline{T}_{cross}$, is

$$\overline{T}_{cross} \approx \frac{1}{t_{cross}} \tag{3.7}$$

The location updating traffic per unit time due to the events 1 and 4 can be approximated by

$$\overline{T}_{start,\,end} \approx \frac{2}{\overline{t}_{trip}} \tag{3.8}$$

where $\overline{t}_{trip} \approx \dfrac{\overline{d}}{v_p}$. ($\overline{d}$ is the mean trip length.)

The total location updating traffic per unit time is then approximated as

$$\overline{T} \approx \overline{T}_{cross} + \overline{T}_{start,\,end} \tag{3.9}$$

For $\overline{v} = 40$ km/hr, $\overline{t}_h = 60$ sec, and $\overline{d} = 100$ km, the location updating traffic values are shown in Figure 3.5.
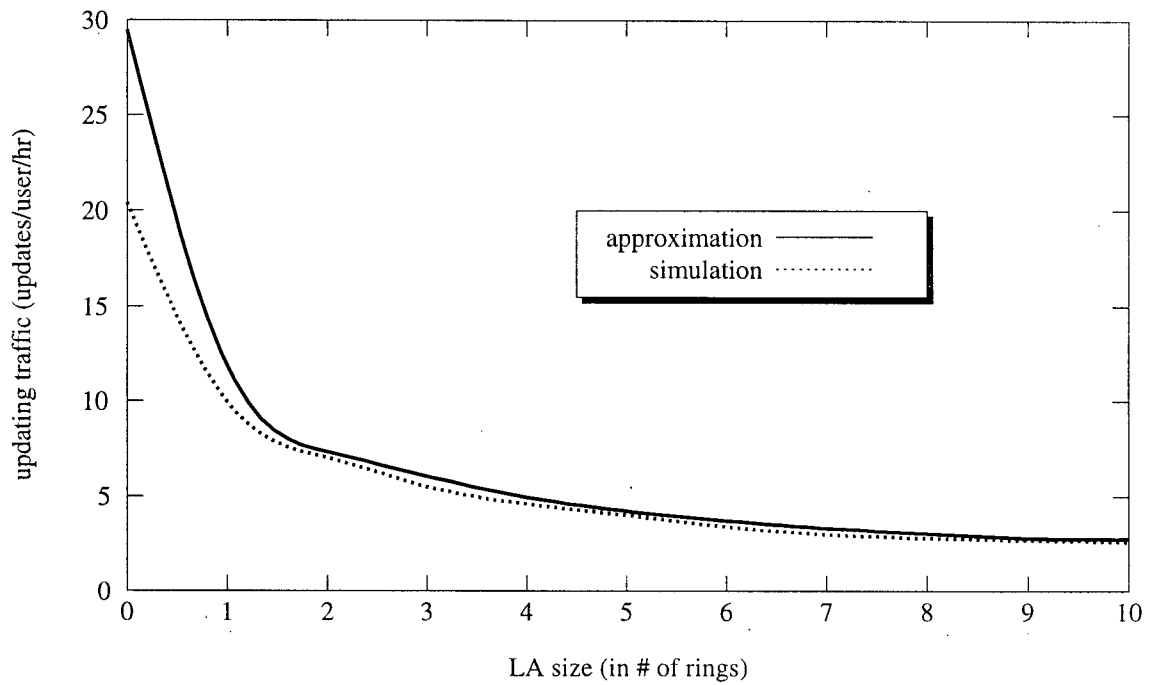
(a)
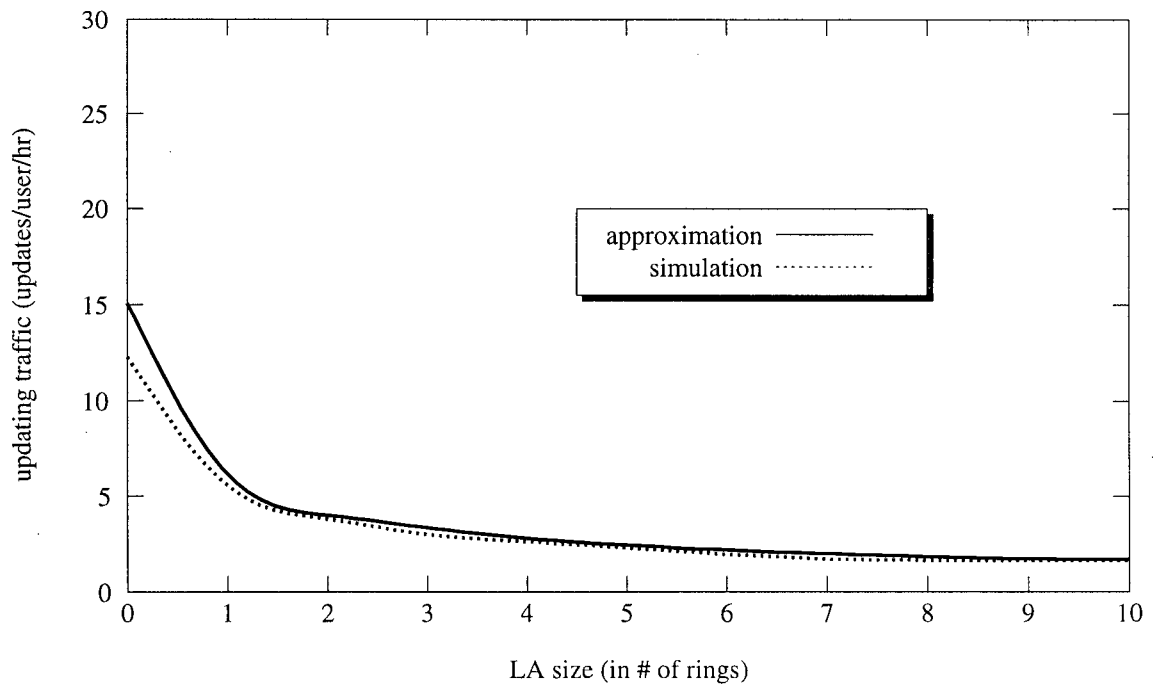
(b)

Figure 3.5 Location updating traffic versus LA size for $\bar{v} = 40$ km/hr, $\bar{t}_h = 60$ sec, and $\bar{d} = 100$ km. (a) $r_{cell} = 1$ km (b) $r_{cell} = 2$ km.

Chapter 4 GENERALIZED LOCATION AREA PAGING SCHEMES

A location area paging scheme is used to page the mobile user in the LA when a call comes in. Based on the location updating scheme described in Chapter 3, the LA each mobile user is currently in is always known to the system. Thus the paging process is always limited to within a LA. The number of cells paged and paging steps needed to find the mobile user are referred to as the *paging traffic* and *paging delay* respectively. In order to minimize the paging delay and paging traffic, an efficient paging scheme is required. The most common and simple paging scheme known as *Flood paging* pages all cells in the LA at once [13]. Although this scheme has the minimum paging delay of 1, it has the maximum paging traffic which equals the number of cells in the LA. Other known paging schemes, such as *Spread paging* and *Selective paging*, try to reduce the paging traffic while keeping the paging delay reasonably low by using a number of paging stages [8]. In this chapter, a more efficient location area paging scheme, called *generalized paging*, is presented.

4.1 Call Arrival Model

A Poisson process with rate λ_{call} arrivals per unit time is used to model call arrivals. The p.d.f. of the inter-call arrival time, $f_{call}(t)$, is exponentially distributed with mean $\frac{1}{\lambda_{call}}$. In oder to analyze the paging scheme performance, the p.d.f., $f_c(t)$, of time between a call arrival and the last location update, t_c, is approximated by simulation [11]. The mean time for a mobile user to exit an LA of radius R from the center of the LA is

$$\bar{t}_R \approx \frac{R}{\bar{v}_p} \tag{4.1}$$

where $\bar{v}_p = \overline{\bar{v}\cos(\phi)}$, mean velocity in the principal direction. Then, f_c is approximated by $\tilde{f}_c$.

$$\tilde{f}_c(t) = \begin{cases} A\lambda_{call}e^{-\lambda_{call}t} & ; \quad 0 \le t \le c \\[2ex] \dfrac{B}{\sqrt{2\pi\sigma_c^2}}e^{-\frac{(t-c)^2}{2\sigma_c^2}} & ; \quad c < t \\[2ex] 0 & ; \quad otherwise \end{cases} \tag{4.2}$$

where

$$A = \frac{1}{1 - e^{-\lambda_{call}\bar{t}_R}} \tag{4.3}$$

$$B = 2[1 - A(1 - e^{-\lambda_{call}c})] \tag{4.4}$$

$$\sigma_c = \frac{B}{A\sqrt{2\pi}\lambda_{call}e^{-\lambda_{call}c}} \tag{4.5}$$

$$c = f(\bar{t}_R)g(\bar{t}_h) \tag{4.6}$$

$$f(\bar{t}_R) = \begin{cases} 0.00023(\bar{t}_R)^2 + 0.4307(\bar{t}_R) - 8.7879 & ; \quad 0 \le \bar{t}_R \le 900 \\ 0.8591\bar{t}_R - 204.8937 & ; \quad 900 \le \bar{t}_R \end{cases} \tag{4.7}$$

$$g(\bar{t}_h) = -0.0016\bar{t}_h + 1.1041 \quad ; \quad 30 \le \bar{t}_h \le 180 \tag{4.8}$$

The simulation and approximate p.d.f.'s of $f_c(t)$ and their goodness of fit are plotted in Figure 4.1

and Figure 4.2 for $\lambda_{call} = 1$ call arrival/hr and $\lambda_{call} = 10$ call arrival/hr.
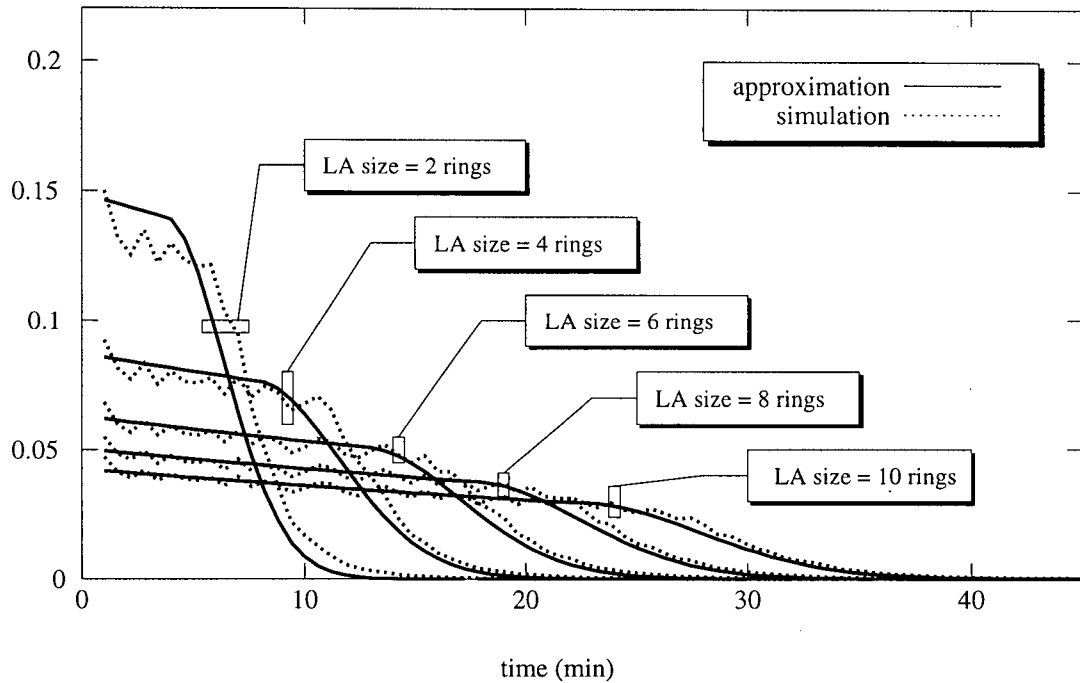
(a)
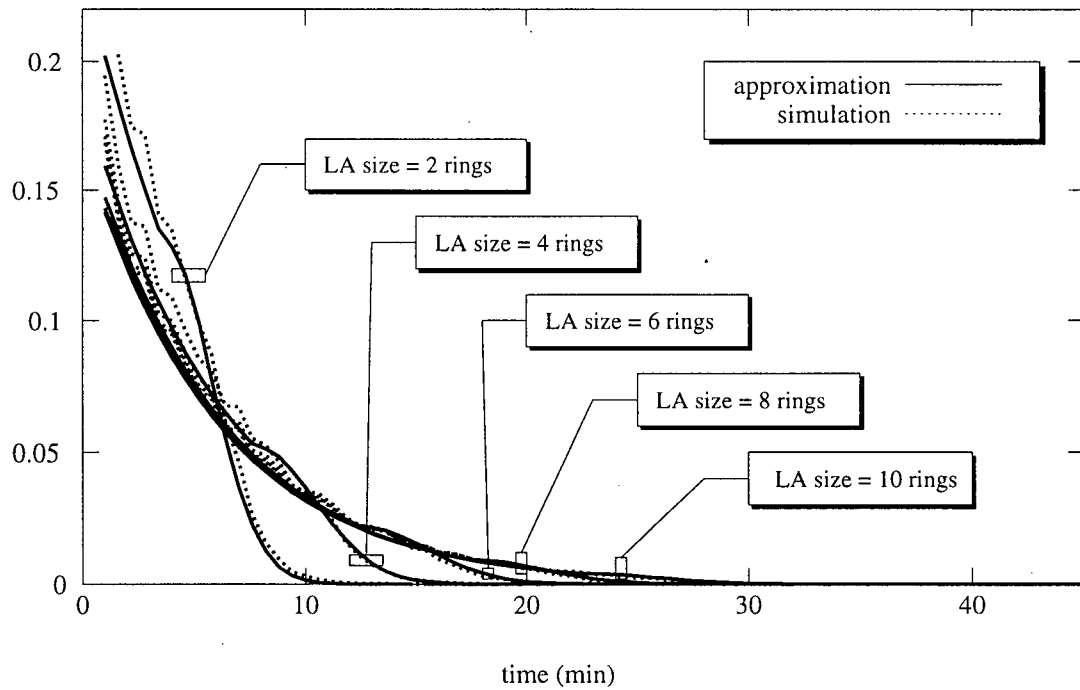
(b)

Figure 4.1 P.d.f.'s of the call arrival time since the last location update for $\bar{v} = 40$ km/hr, $\bar{t}_h = 60$ sec, and $r_{cell} = 1$ km. (a) $\lambda_{call} = 1$ call arrival/hr. (b) $\lambda_{call} = 10$ call arrival/hr.
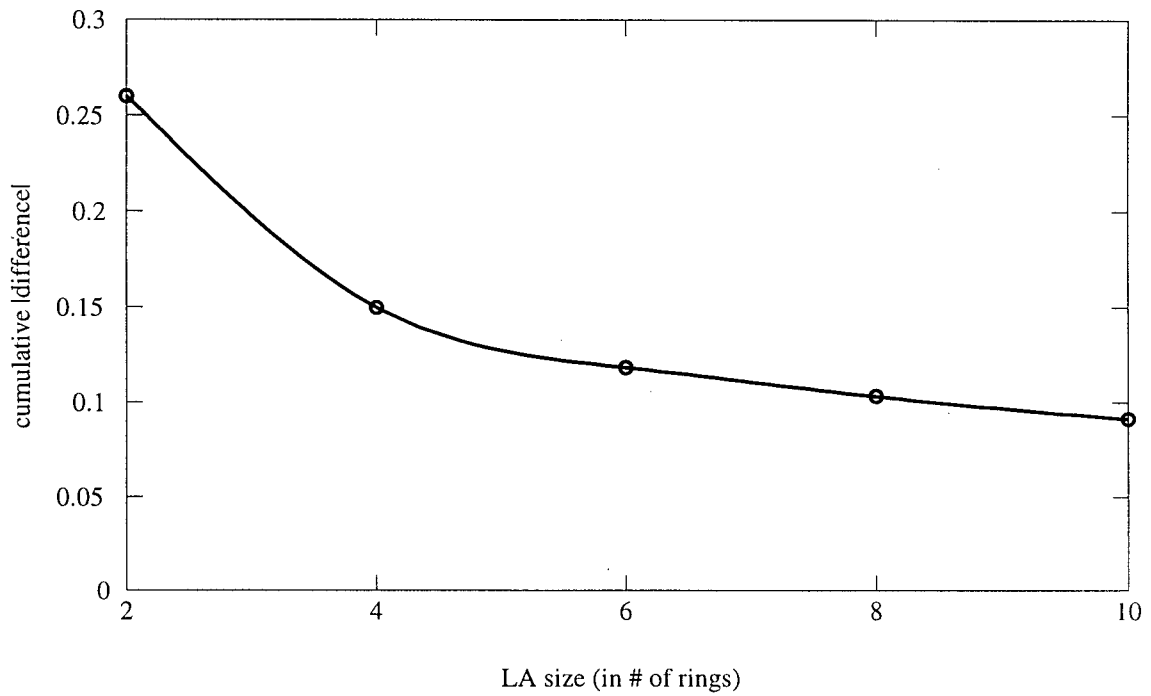
(a)
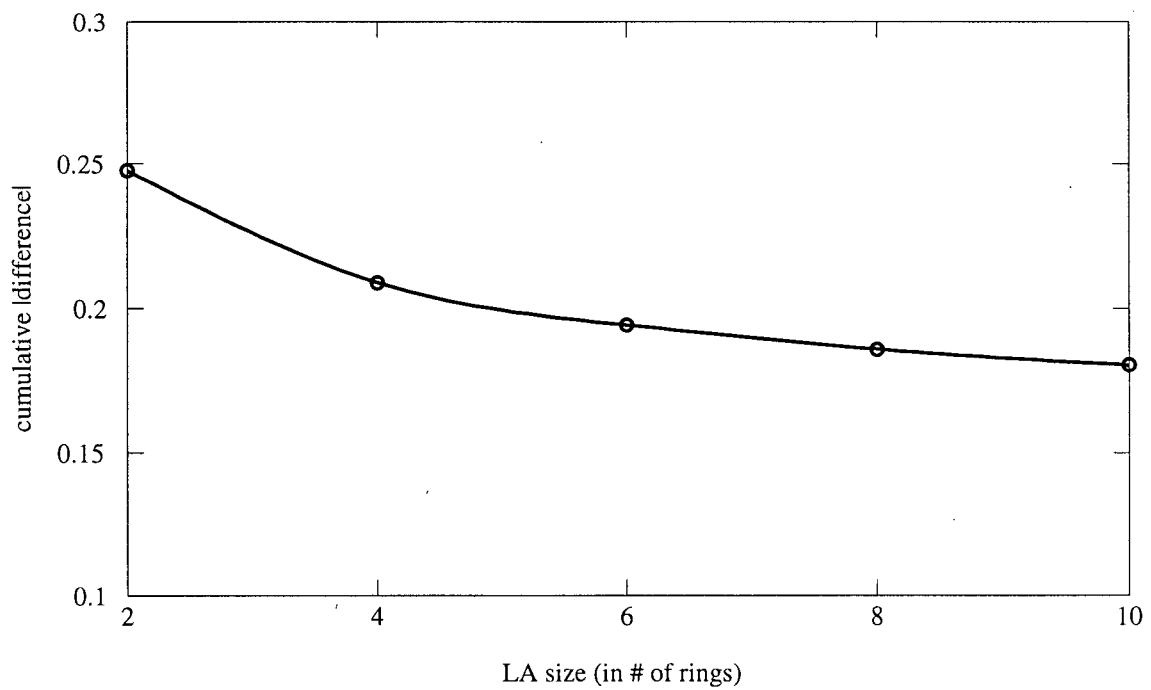
(b)

Figure 4.2 Goodness of fit of the approximate $f_c(t)$ p.d.f. for $\bar{v}$ = 40 km/hr, i_h = 60 sec, and r_{cell} = 1 km. (a) λ_{call} = 1 call arrival/hr. (b) λ_{call} = 10 call arrival/hr.

4.2 Cell Numbering Notation

A notation to identify each cell in the LA is described in this section. Two numbers, i and j, will be used to identify each cell in the LA. The i, $0 \leq i \leq LAsize$, will denote the ring number in the LA and the j, $0 \leq j \leq [N(i) - N(i-1)]$, will denote the cell number in the ith ring. As shown in Figure 4.3, the first cell above the starting line in each ring will be given the cell number of 0 and the rest of the cells in each ring will have sequentially increasing cell numbers in the counter-clockwise direction. From now on, a cell will be denoted as *cell(i,j)*.

starting line, 0°
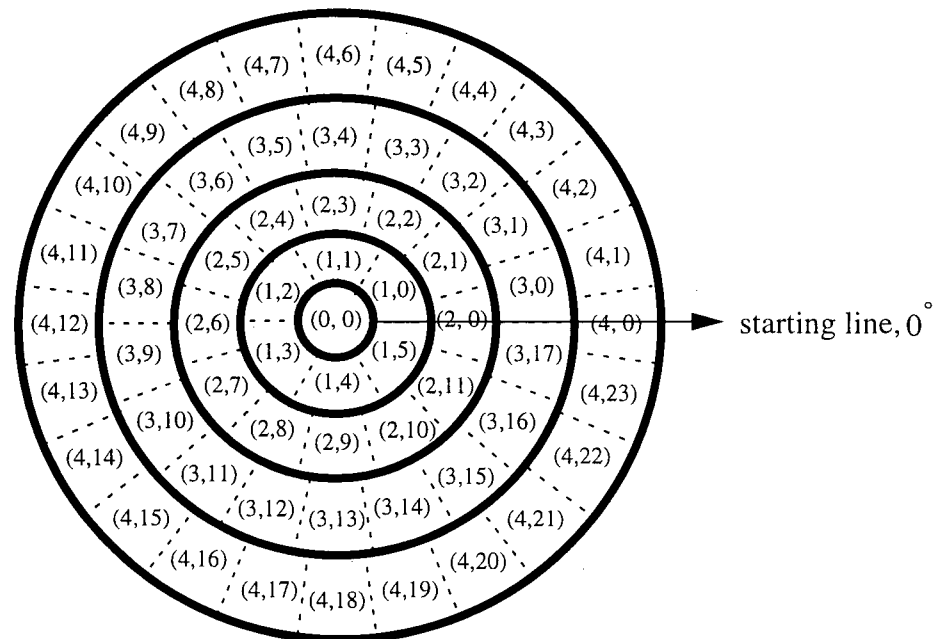
Figure 4.3 Numbering of cells in an LA of size = 4.

4.3 LA Ring Probability

The ring probability refers to the probability that a user is in a particular ring in its registered LA at a particular time. To estimate the ring probabilities, the p.d.f. of the radial distance, r, of a mobile user at time t is used. Because the mobile user must be inside the LA, the

p.d.f. of the radial distance obtained in Section 2.3.1 is limited by the condition that the user has not exited the LA. If the LA size is R, this p.d.f. is given by

$$f_R(r|t, withinLA) = f_R(r|t, r < R_{eqv}(R))$$

$$= \frac{f_R(r|t)}{\int_0^{R_{eqv}(R)} f_R(\xi|t) \, d\xi} \tag{4.9}$$

In Section 3.2, the equivalent distance for each ring in an LA is defined. Using Eqn. (3.3), i^{th} ring's width can be expressed as $R_{eqv}(i) - R_{eqv}(i-1)$. Then the ring probability for i^{th} ring at time t is given by

$$P_{ring}(i, t) \approx \int_{R_{eqv}(i-1)}^{R_{eqv}(i)} f_R(r|t, withinLA) \, dr \tag{4.10}$$

4.4 LA Angular Probability

The angular probability refers to the probability that a user is in a particular angular sector in its registered LA at a particular time. From (3.4), we know the ith ring in the LA has [$N(i)$-$N(i-1)$] cells in it. Thus the ith ring can be divided into [$N(i)$-$N(i-1)$] equal sectors, which correspond to cells, and the angular probability for *cell(i,j)* at time t can be estimated using the angular deviation p.d.f. of the mobile user at time t, $f_\Theta(\theta|t)$, in Section 2.3.2 as

$$P_{ang}(i, j, t) = \int_{\Theta_{i,j}} f_\Theta(\theta|t) \, d\theta \tag{4.11}$$

where $\Theta_{i,j}$ corresponds to the angular range covering cell(i,j).

4.5 LA Cell Probability

A cell probability refers to the probability of a user being in a given cell in the LA. The cell probability for each cell at time t can be approximated by a product of the cell's ring probability and the angular probability as shown in Figure 4.4. Then the cell probability for *cell(i, j)* at time t_e can be expressed as

$$P_{cell}(i, j, t_e) = P_{ring}(i, t_e) \cdot P_{ang}(i, j, t_e) \qquad (4.12)$$

where t_e is the elapsed time since the last location update.
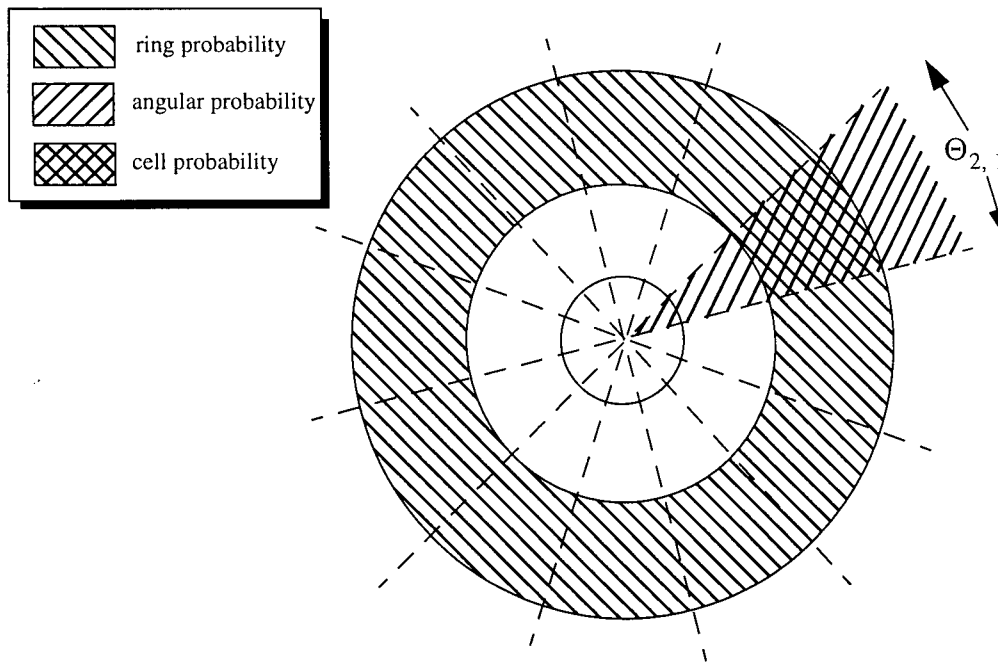
Figure 4.4 Cell probability illustration for *cell*(2,1)

4.6 Review of Other Paging Schemes

In this section, three paging schemes, *Flood paging*, *Spread paging*, and *Selective paging*, are described. In *Flood paging*, when a call comes in for a user, all the cells in the user's registered LA are paged simultaneously. Thus, it has the minimum average paging delay of 1, but it also has the highest possible average paging traffic. In *Spread paging*, the system pages the center ring (cell) first. If the user is not found, the next rings, starting from the 1st ring, are paged in order. Since the inner rings contain less cells, *Spread paging* tries to reduce the number of cells paged by paging the rings with fewer cells first. In *Selective paging*, the ring probabilities are evaluated as described in Section 4.3. When a call comes in for a user, the system pages the ring with the highest probability first. If the user is not found, the ring with the second highest probability is paged and so on until the user is found.

4.7 Generalized Paging Schemes

In this section, two new paging schemes, called *generalized paging scheme with time-stamp and generalized paging scheme without time-stamp,* are described. For convenience, we will refer to *generalized paging scheme with time-stamp* as *Scheme A* and *generalized paging scheme without time-stamp* as *Scheme B* from now on. Using the directional random walk mobility model and the location updating scheme described in Chapter 2 and 3, the cell probabilities in the LA are estimated. Then cells in the LA are grouped into a number of subsets, N_S, according to their cell probabilities. We will have two different ways of grouping cells into subsets. The first way to group the cells is that, for each subset, a threshold parameter, p_i, is used to select its member cells. The cells with the highest cell probabilities are added to the first subset until the sum of their cell probabilities reaches the first threshold parameter. The next cells are

added to the second subset until the sum of their cell probabilities and the first parameter reaches the second parameter. This process continues until all cells are grouped into the subsets. The second way to group the cells is choosing a fixed number of cells in a subset. All subsets will have an equal number of cells, N_c, in them.

4.7.1 With location update time-stamp (*Scheme A*)

We assume that the time of the location update is registered with the system. The time, t_e, between the call arrival and the last location update is used to estimate the user's current location and to select the cells to be paged. When a call comes in, we evaluate all cells' cell probability estimates at t_e given by Eqn. (4.12). Assuming an LA size of R, let $\mathbf{P}_{\text{cell}}(t_e)$ be a vector containing the estimates of cell probabilities, i.e.

$$\mathbf{P}_{\text{cell}}(t_e) = \begin{bmatrix} P_{cell}(0, 0, t_e) \\ P_{cell}(1, 0, t_e) \\ P_{cell}(1, 1, t_e) \\ \cdot \\ \cdot \\ P_{cell}(R, 6R-1, t_e) \end{bmatrix} \tag{4.13}$$

Then $\mathbf{P}_{\text{cell}}(t_e)$ is sorted in descending order (highest probability as first element) to yield the vector $\mathbf{P}^{S}_{\text{cell}}(t_e)$ and the cells in $\mathbf{P}^{S}_{\text{cell}}(t_e)$ are divided into subset vectors, $\mathbf{P}^{S}_{\text{cell}, 0}(t_e)$, $\mathbf{P}^{S}_{\text{cell}, 1}(t_e)$, $\mathbf{P}^{S}_{\text{cell}, 2}(t_e)$, ... , and $\mathbf{P}^{S}_{\text{cell}, N_s}(t_e)$. For the first way of grouping cells, cells are grouped such that,

$$sum(\mathbf{P}^{\mathbf{S}}_{\text{cell}, i}(t_e)) \le (p_i - p_{i-1}) \tag{4.14}$$

where $sum(\mathbf{X})$ represents the sum of $\mathbf{X}$'s elements and $i \ge 0$. For the second way of grouping

cells, the first N_c cells in $\mathbf{P}^{\mathbf{S}}_{\text{cell}}(t_e)$ are put into the first subset vector and the next N_c cells are put

into the second vector and so on.

If the user is in a cell which belong to the ith subset vector, $\mathbf{P}^{\mathbf{S}}_{\text{cell}, i}$, the paging delay is $i+1$.

Therefore, the average paging delay at time t_e is

$$\overline{D}(t_e) = \begin{bmatrix} 1 & 2 & \dots & N_S + 1 \end{bmatrix} \times \mathbf{P}_{\text{s}}(t_e). \tag{4.15}$$

where

$$\mathbf{P}_{\text{s}}(t_e) = \begin{bmatrix} sum(\mathbf{P}^{\mathbf{S}}_{\text{cell}, 0}(t_e)) \\ sum(\mathbf{P}^{\mathbf{S}}_{\text{cell}, 1}(t_e)) \\ \cdot \\ \cdot \\ sum(\mathbf{P}^{\mathbf{S}}_{\text{cell}, N_S}(t_e)) \end{bmatrix} \tag{4.16}$$

Averaging $\overline{D}(t_e)$ using the call arrival p.d.f., $f_c(t)$, we obtain the average paging delay as

$$\overline{D} = \int_0^{\infty} \overline{D}(t) f_c(t) dt. \tag{4.17}$$

If the user is in a cell which is in the ith subset, the paging traffic is the total number of

cells in 0 through i^{th} subset. Then the average paging traffic at time t_e is

$$\bar{T}(t_e) = \left[\mathbf{N}^s_{cell}(t_e) \right]^T \times \begin{bmatrix} 1 & 1 & \cdots & 1 \\ 0 & 1 & \cdots & 1 \\ \cdot & \cdot & \cdot & \cdot \\ \cdot & \cdot & \cdot & \cdot \\ 0 & \cdots & 0 & 1 \end{bmatrix} \times \mathbf{P}_s(t_e) \qquad (4.18)$$

where $\begin{bmatrix} \cdot \end{bmatrix}^T$ is the transpose operation and $\mathbf{N}^s_{cell}(t_e)$ is a vector whose i^{th} component is the number of cells in i^{th} subset.

The average paging traffic is obtained by averaging $\bar{T}(t_e)$ using the call arrival p.d.f., i.e.

$$\bar{T} = \int_0^\infty \bar{T}(t) f_c(t) dt. \qquad (4.19)$$

4.7.2 Without location update time-stamp (*Scheme B*)

In this section, it is assumed that the time of the location update is not registered with the system. Thus, when the location update occurs, only the mobile user's current cell information is known. Then the estimates of cell probabilities do not depend on the elapsed time, t_e, since the last location update. When a call comes in for a user, the same sets of cells are paged in the same order without considering t_e. The cell probability estimate for *cell(i, j)* can be expressed as

$$P_{cell}(i, j) = P_{ring}(i) \cdot P_{ang}(i, j) \qquad (4.20)$$

where

$$P_{ring}(i) = \int_{0}^{\infty} P_{ring}(i, t) f_c(t) dt \qquad (4.21)$$

and

$$P_{ang}(i, j) = \int_{0}^{\infty} P_{ang}(i, j, t) f_c(t) dt \qquad (4.22)$$

Assuming an LA size of R, let $\mathbf{P}_{cell}$ be a vector containing the cell probability estimates, i.e.

$$\mathbf{P}_{cell} = \begin{bmatrix} P_{cell}(0, 0) \\ P_{cell}(1, 0) \\ P_{cell}(1, 1) \\ \cdot \\ \cdot \\ P_{cell}(R, 6R - 1) \end{bmatrix} \qquad (4.23)$$

Then $\mathbf{P}_{cell}$ is sorted in descending order (highest probability as first element) to yield the vector $\mathbf{P}_{cell}^{S}$ and the cells in $\mathbf{P}_{cell}^{S}$ are divided into subset vectors, $\mathbf{P}_{cell, 0}^{S}$, $\mathbf{P}_{cell, 1}^{S}$, $\mathbf{P}_{cell, 2}^{S}$, ... , and $\mathbf{P}_{cell, N_s}^{S}$. For the first way of grouping cells, the cells are grouped such that,

$$sum(\mathbf{P}_{cell, i}^{S}) \le (p_i - p_{i-1}) \qquad (4.24)$$

, where $sum(\mathbf{X})$ represents the sum of $\mathbf{X}$'s elements and $i \ge 0$. For the second way of grouping cells, the first N_c cells in $\mathbf{P}_{cell}^{S}$ are put into the first subset vector, the next N_c cells are put into the second vector and so on.

If the user is in a cell which belong to the ith subset vector, $\mathbf{P}^{\mathbf{S}}_{\text{cell},\,i}$, the paging delay is $i+1$.

Therefore, the average paging delay is

$$\overline{D}(t_e) = \begin{bmatrix} 1 & 2 & \dots & N_S + 1 \end{bmatrix} \times \mathbf{P}_{\mathbf{s}}.$$ (4.25)

where

$$\mathbf{P}_{\mathbf{s}} = \begin{bmatrix} sum(\mathbf{P}^{\mathbf{S}}_{\text{cell},\,0}) \\ sum(\mathbf{P}^{\mathbf{S}}_{\text{cell},\,1}) \\ . \\ . \\ sum(\mathbf{P}^{\mathbf{S}}_{\text{cell},\,N_s}) \end{bmatrix}$$ (4.26)

If the user is in a cell which is in the ith subset, the paging traffic is the total number of

cells in 0 through i^{th} subset. Then the average paging traffic is

$$\overline{T} = \begin{bmatrix} \mathbf{N}^{\mathbf{s}}_{\text{cell}} \end{bmatrix}^T \times \begin{bmatrix} 1 & 1 & \dots & 1 \\ 0 & 1 & \dots & 1 \\ . & . & . & . \\ . & . & . & . \\ 0 & \dots & 0 & 1 \end{bmatrix} \times \mathbf{P}_{\mathbf{s}}$$ (4.27)

where $\begin{bmatrix} . \end{bmatrix}^T$ is the transpose operation and $\mathbf{N}^{\mathbf{s}}_{\text{cell}}$ is a vector whose i^{th} component is the

number of cells in i^{th} subset.

4.8 Numerical Results

The two *generalized paging* schemes' simulation and approximation results are presented in this section. For the simulation results, a user travels toward a destination (at infinite distance) from the center of an LA following the directional random walk model in Section 2.1. As the user crosses an LA boundary or receives a call (Section 4.1), his location is updated using the dynamic LA-based location updating model described in Section 3.3. When a call comes in, the user is paged based on the cell probabilities obtained as follows:

For *Scheme A*, the user is allowed to travel toward the destination for certain durations of time (e.g. 1 minute, 2 minutes, 3 minutes and etc.). Then we note the user's locations within an LA at these different times. We ignore the user's location if he has exited the LA. From these statistics, the cell probability sets for different times are calculated.

For *Scheme B*, the user's location within an LA is noted whenever a call comes in for the user. From these statistics, the cell probabilities are calculated.

For the approximate results, the cell probabilities are estimated and the paging performances are evaluated as described in Section 4.7.1 for *Scheme A* and in Section 4.7.2 for *Scheme B*.

The paging schemes' performances are measured in terms of their average paging delays and traffics. The proposed two *generalized paging schemes* are compared to *Flood paging*, *Spread paging*, and *Selective paging*. A mean speed of 40 km/hr, mean velocity hold time of 60 sec, cell radius of 1 km, and call arrival rate of 1 call/hr are assumed.

4.8.1 Performance comparison

The performance of *Flood paging*, *Spread paging*, and *Selective paging* are shown in Figure 4.5. Although *Flood paging* has the smallest average paging delay of 1, it has the largest possible average paging traffic. *Spreading paging*'s average paging delay and traffic are always higher than those of *Selective paging*. With an LA size of 10, *Selective paging*'s average paging delay and traffic are only about 35% and 55% of *Spreading paging*'s average paging delay and traffic. *Selective paging* outperforms *Spreading paging*, and it will be used as the reference when showing the performances of two *generalized paging schemes*.

Figure 4.6 shows the performances of the two *generalized paging schemes* using a fixed number for each LA size to group cells into subsets. By trying out different fixed number of cells to form subsets, we found that using the numbers, 3, 4, 5, 6, 7, 8, 10, 13, 16, and 20 as the N_c's for the LA sizes, 1, 2, 3, 4, 5, 6, 7, 8, 9, and 10, results in reasonably low average paging delay values that are close to 1 and significantly lower average paging traffic values than other paging schemes. We can see that the average paging delay and traffic are always lower than those of *Selective paging scheme*. For an LA size of 10, the average paging delay and traffic are reduced by about 45% and 65% when *Scheme A* is used instead of *Selective paging* and by about 35% and 55% when *Scheme B* is used. When Scheme B is compared to *Scheme A*, we can see *Scheme A* always performs better. With an LA size of 10, *Scheme A*'s average paging delay and traffic are about 15% lower than those of *Scheme B*.

Selective paging, *Scheme A*, and *Scheme B* are also compared with changes in parameter values in Figures 4.7, 4.8, and 4.9. The mean speed ($\bar{v}$), mean velocity hold time ($\bar{t_h}$), and call
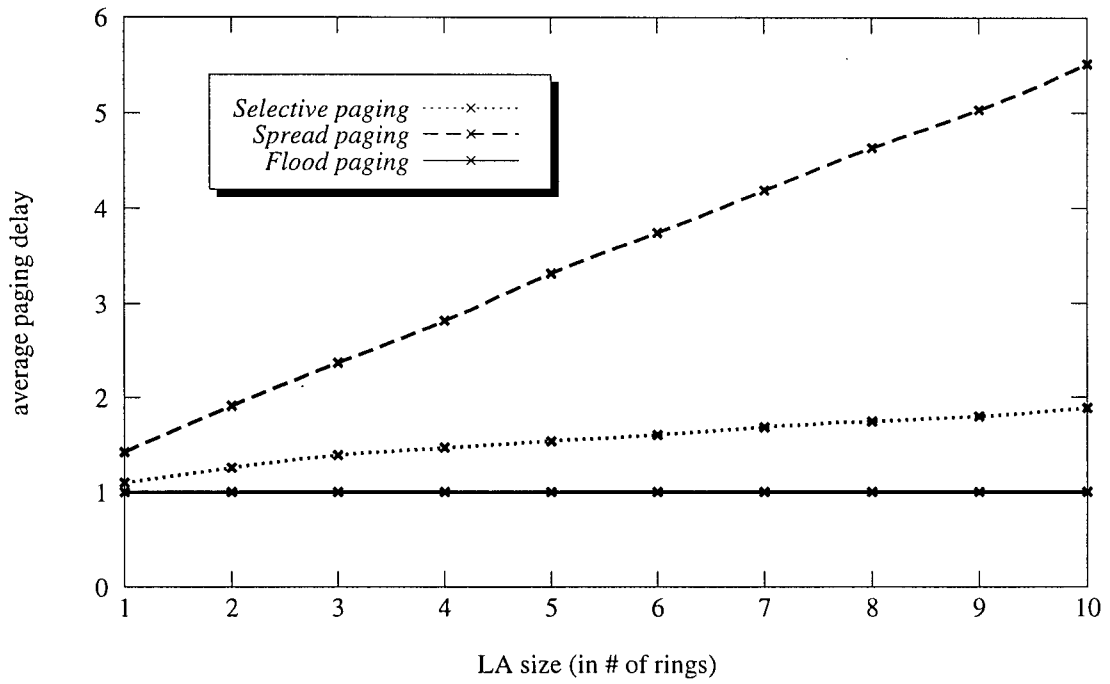
(a)
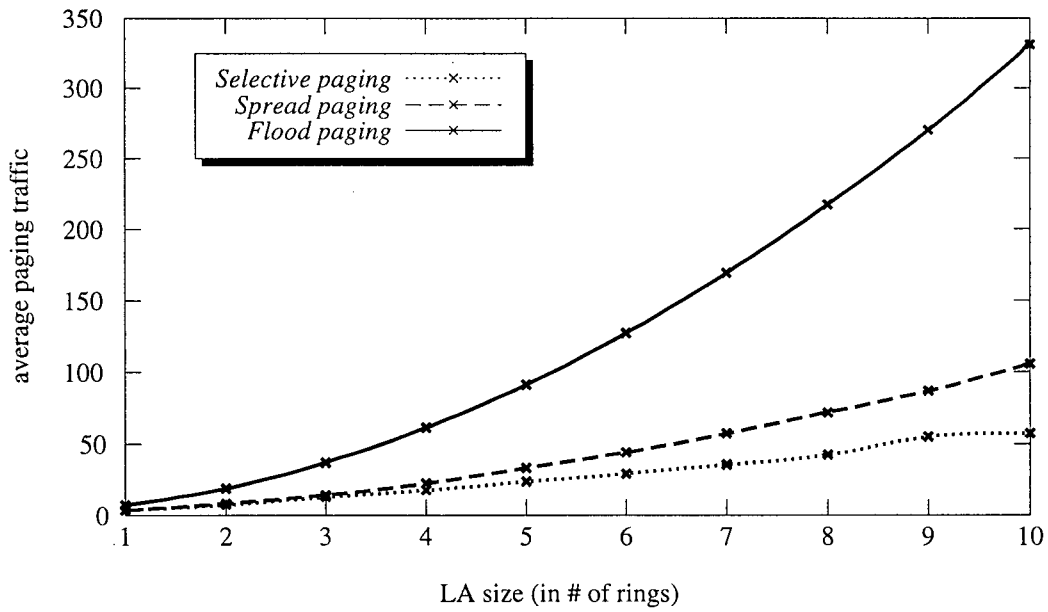
(b)

Figure 4.5 Performance of *Flood paging*, *Spreading paging*, and *Selective paging* with $\bar{v} = 40$ km/hr, $\overline{t_h} = 60$ sec, $r_{cell} = 1$ km, and $\lambda_{call} = 1$ call/hr. (a) average paging delay. (b) average paging traffic.
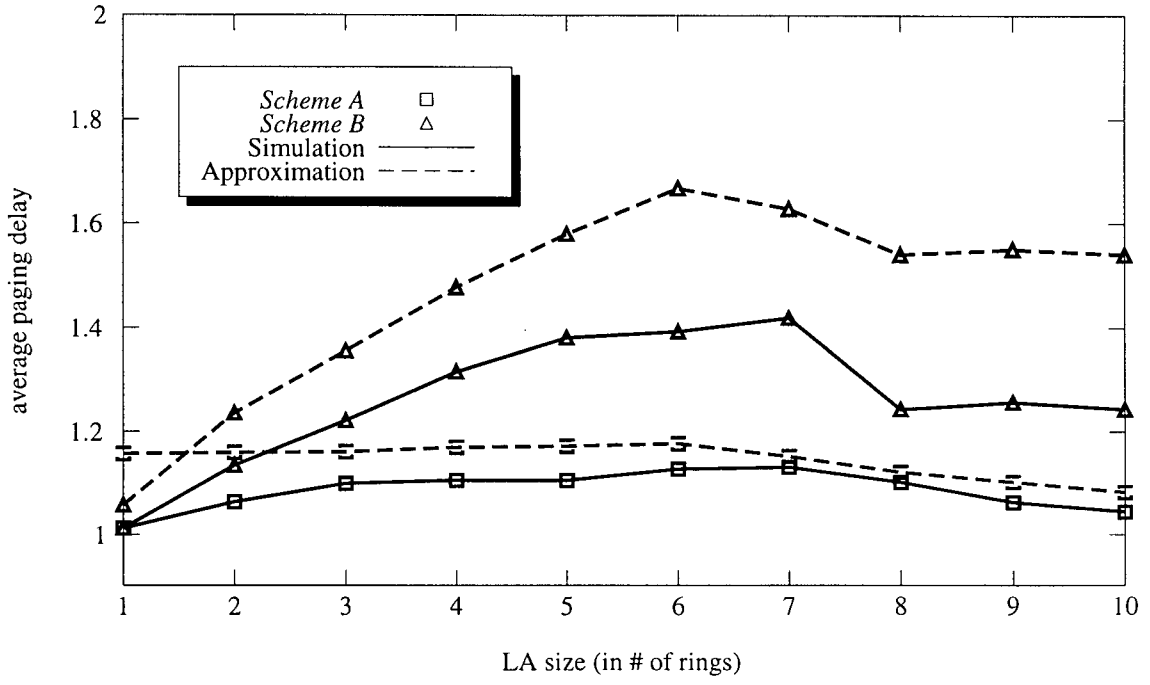
(a)
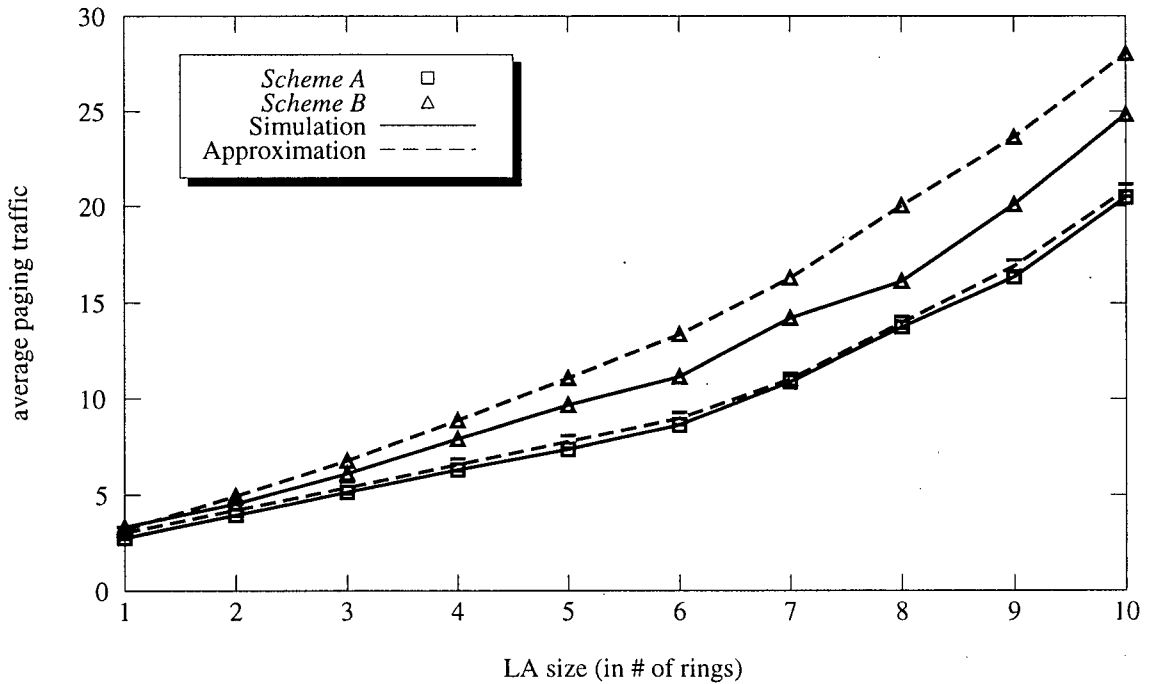
(b)

Figure 4.6 Performance of *Scheme A* and *Scheme B* with $\bar{v}$ = 40 km/hr, $\bar{t}_h$ = 60 sec, r_{cell} = 1 km, and λ_{call} = 1 call/hr. (a) average paging delay. (b) average paging traffic.

arrival rate (λ_{call}) are changed one parameter at a time while the other two parameters are fixed at the reference values ($\bar{v}$ = 40 km/hr, $\bar{t_h}$ = 60 sec, and λ_{call} = 1 call/hr). The simulation values are obtained for the LA sizes of 2, 6, and 10. The three figures all show that *Scheme A* and *Scheme B* (*Scheme A*, in particular) perform better than *Selective paging* in terms of average paging delay and traffic. Also, *Scheme A* and *Scheme B* are not very sensitive to changes in parameter values.

4.8.2 Trade-off between average paging delay and traffic

In the *generalized paging* schemes, we can control the number of cells in each subset by either selecting different threshold parameter values or fixed number of cells for each subset. As the number of cells in each subset increases, we can expect the average paging delay to decrease and the average paging traffic to increase. On the other hand, as the number of cells in each subset decreases, it is expected that the average paging delay will increase and the average paging traffic will decrease. Figure 4.10 shows the relationships between the average paging delay and traffic values for *Scheme* A and *Scheme B*. Several different sets of 4 threshold parameters (p_1, p_2, p_3, and p_4) are used, along with different fixed numbers (N_c) of cells for each paging subset. It can be seen that using the threshold parameters to group cells into subsets does not show any improvements over using a fixed number of cells for each subset. It is also noted that *Scheme A* always outperforms *Scheme B*, no matter how many cells are grouped into each subset.

By controlling the number of cells in each subset, the system can adjust its paging performance to satisfy different requirements. For example, if the average paging delay is more important than the average paging traffic, the system can increase the number of cells and decrease the average paging delay and vice versa.
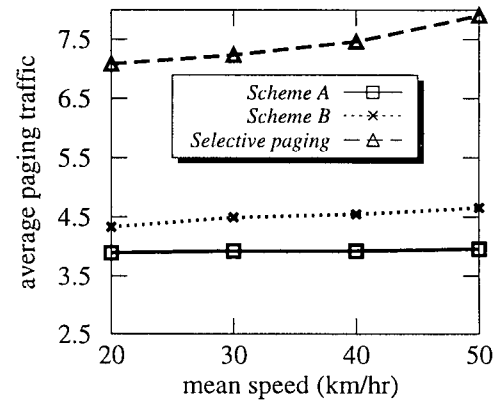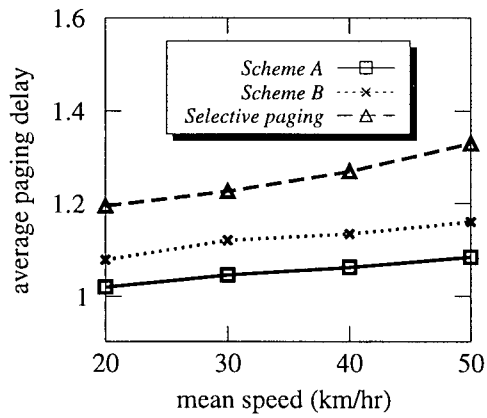
(a)
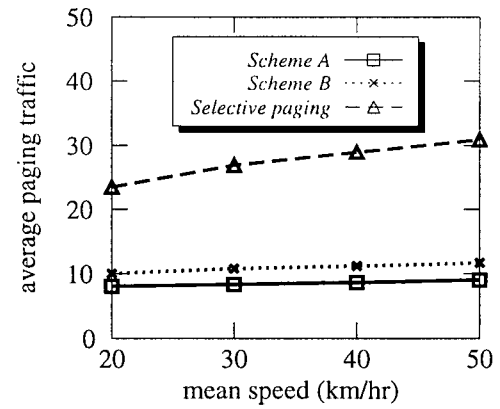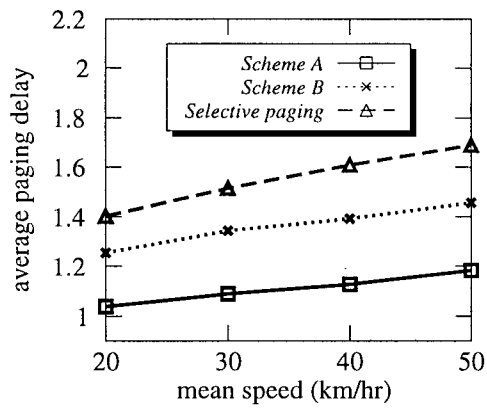
(b)
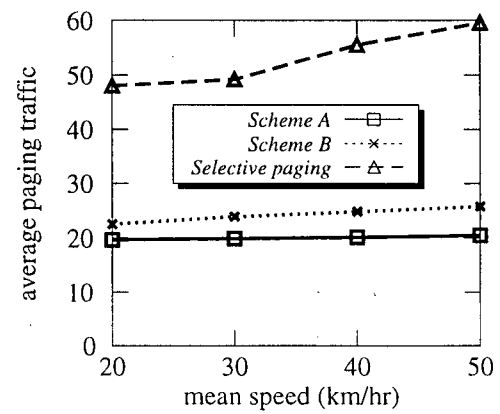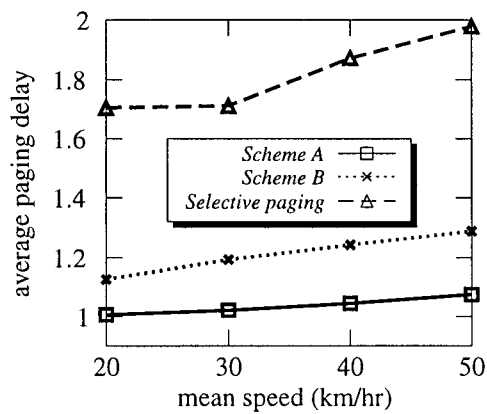
(c)

Figure 4.7 Performance of *Selective paging*, *Scheme A*, and *Scheme B* versus the user mean speed for $\bar{t}_h = 60$ sec, $\lambda_{call} = 1$ call/hr, and $r_{cell} = 1$ km. (a) LA size = 2. (b) LA size = 6. (c) LA size = 10.

(a)

(b)

(c)
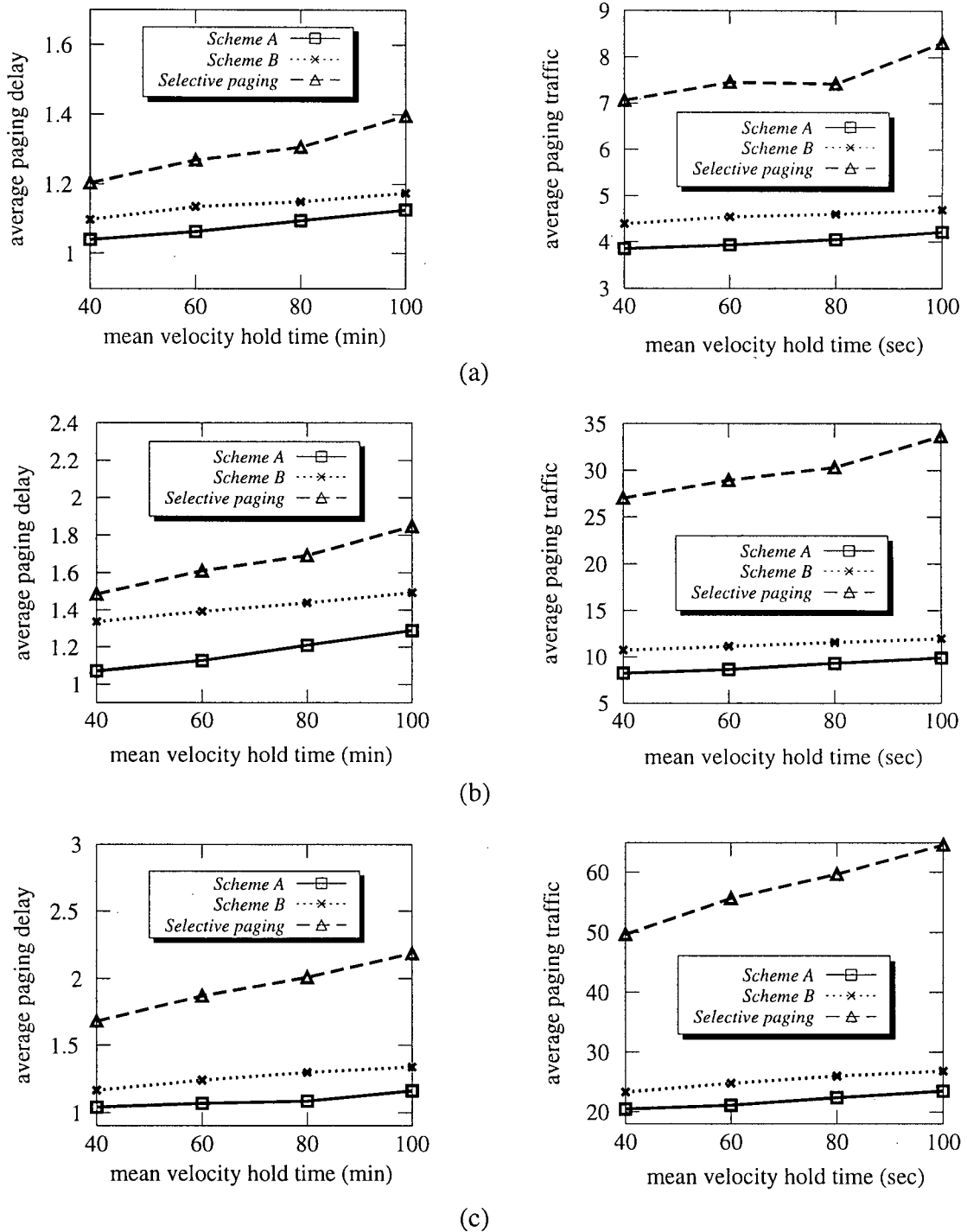
Figure 4.8 Performance of *Selective paging*, *Scheme A*, and *Scheme B* versus the mean velocity hold time for $\bar{v} = 40$ km/hr, $\lambda_{call} = 1$ call/hr, and $r_{cell} = 1$ km. (a) LA size = 2. (b) LA size = 6. (c) LA size = 10.
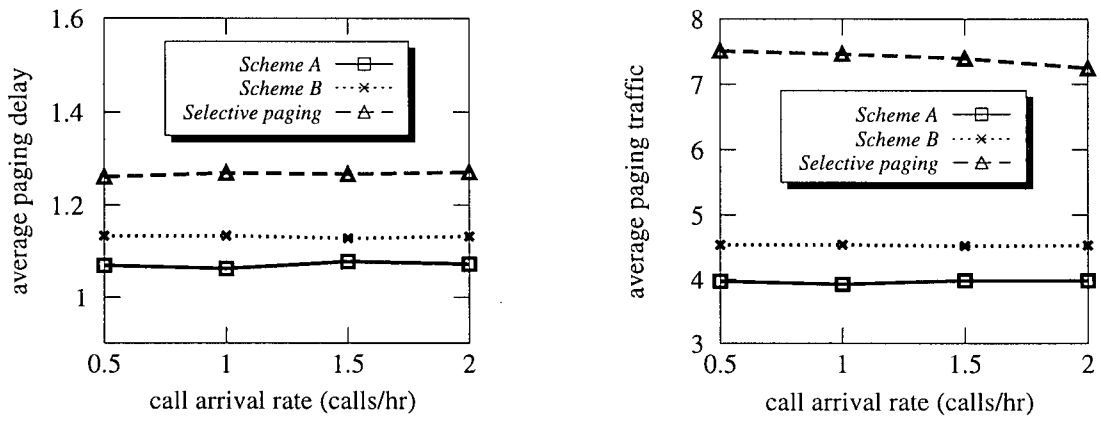
(a)
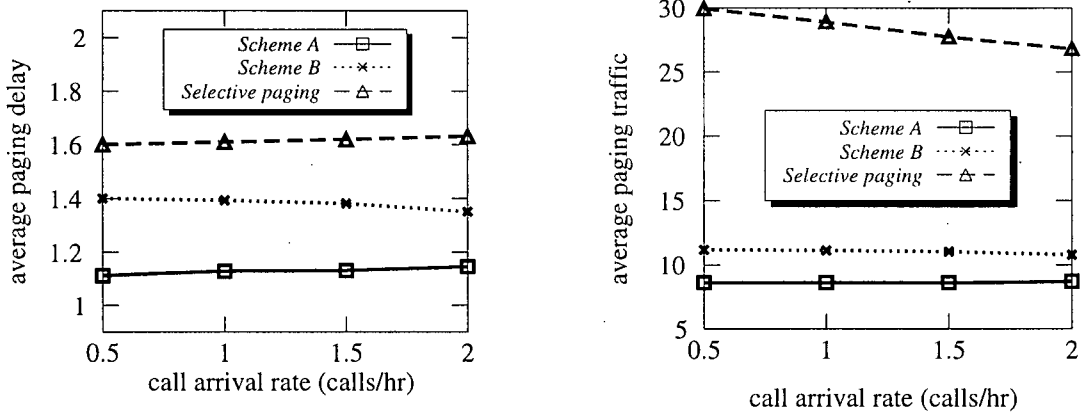
(b)
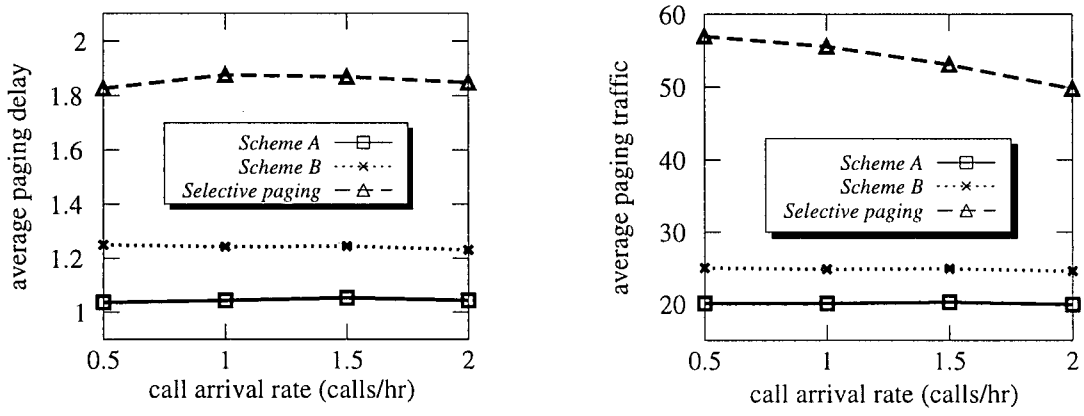
(c)

Figure 4.9 Performance of *Selective paging*, *Scheme A*, and *Scheme B* versus the call arrival rate for $\bar{v}$ = 40 km/hr, $\overline{t_h}$ = 60 sec, and r_{cell} = 1 km. (a) LA size = 2. (b) LA size = 6. (c) LA size = 10.

(a)

(b)
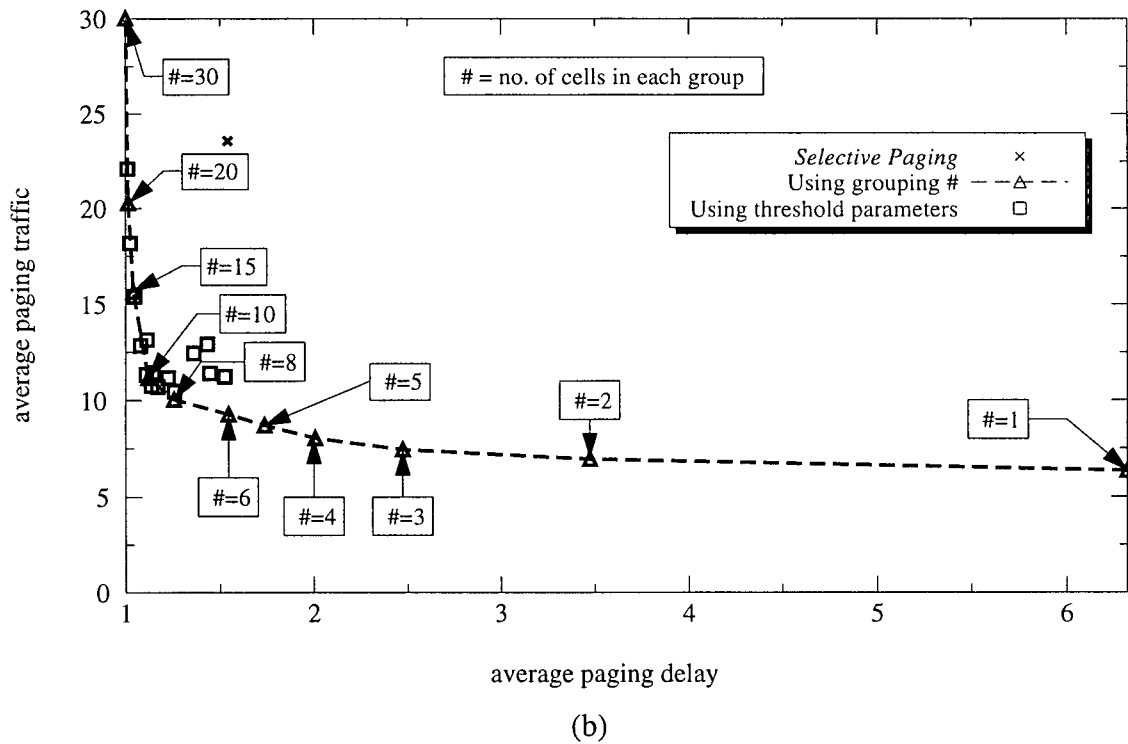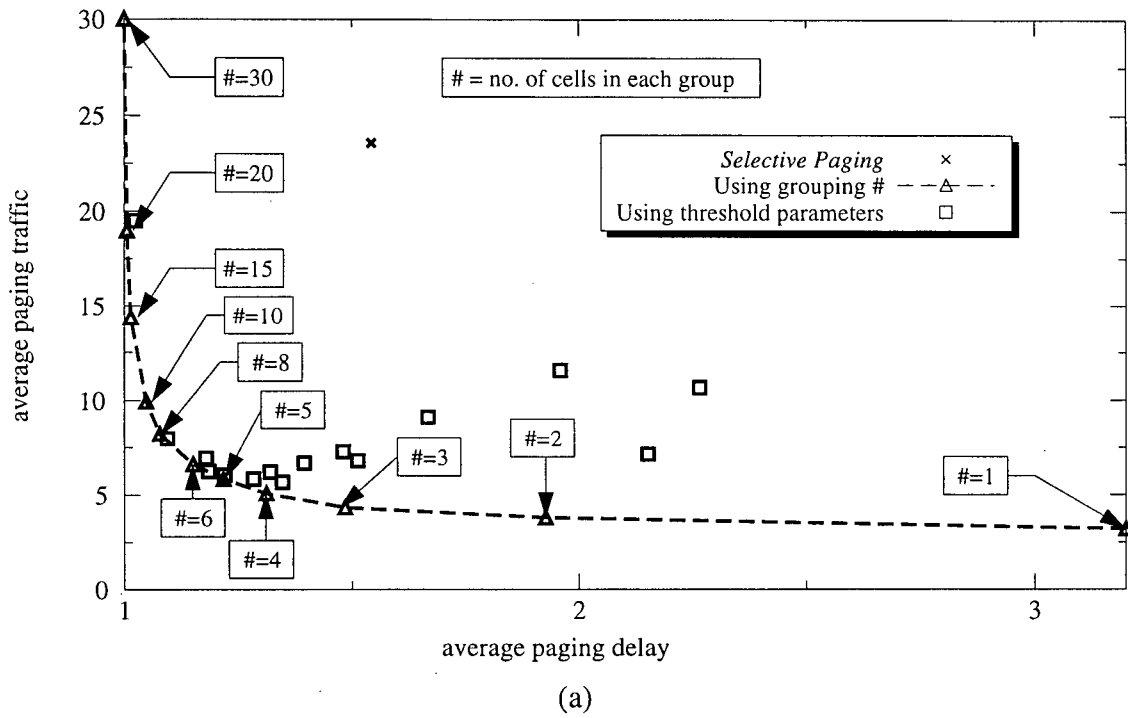
Figure 4.10 Average paging traffic versus average paging delay with $\bar{v}$ = 40 km/hr, $\bar{t_h}$ = 60 sec, λ_{call} = 1 call/hr, LA size = 5, and r_{cell} = 1 km. (a) *Scheme A*. (b) *Scheme B*.

4.9 Verification of LA Entry Point Assumption

So far, when a user has crossed an LA boundary, we repositioned the user back to the center of the new LA. We assumed that a user always starts his journey at the center of the LA center cell. In this section, we show that this assumption is valid and the *generalized paging schemes'* performances are not affected significantly by this assumption. For instance, we choose the left most corner of a cell as the new LA entry point. When a user crosses an LA boundary, we assume that the user will continue his journey from this point, instead of the center of a cell. Figure 4.11 shows the performance of *Scheme A* with the new LA entry point. We see that the performance of *Scheme A* is not affected much by a different LA entry point. As the LA size increases, the difference in performance decreases. For LA size > 4, the differences in average paging delays and traffics are within ±5% of the original values. This also holds for *Scheme B*.
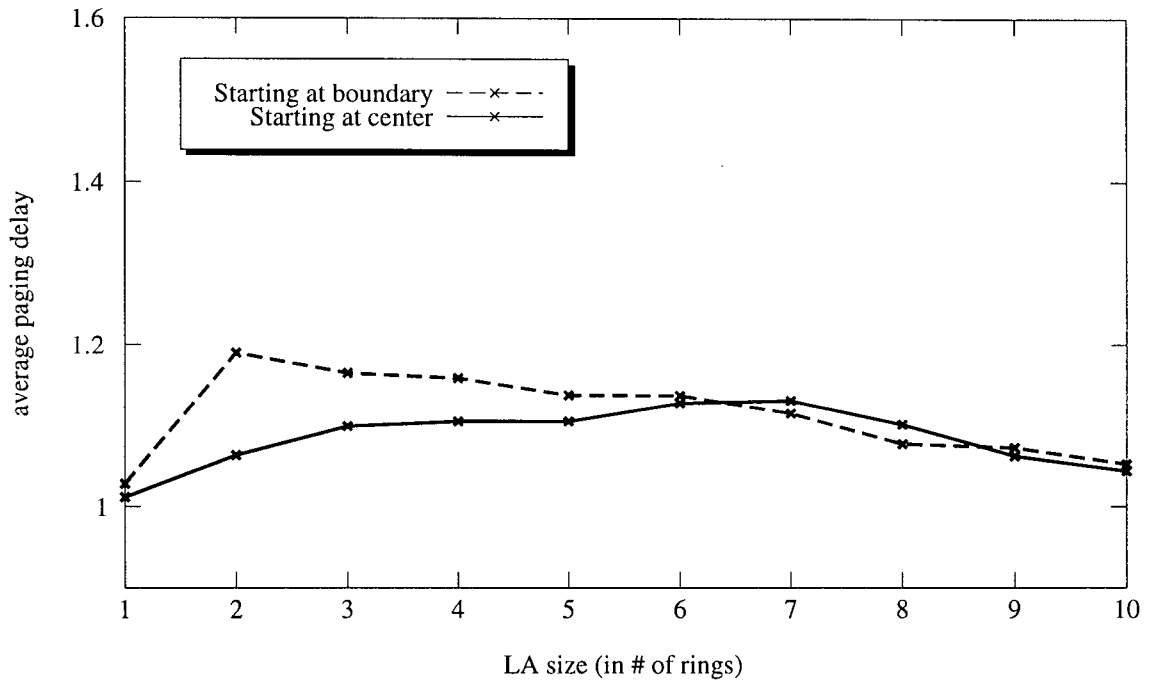
(a)
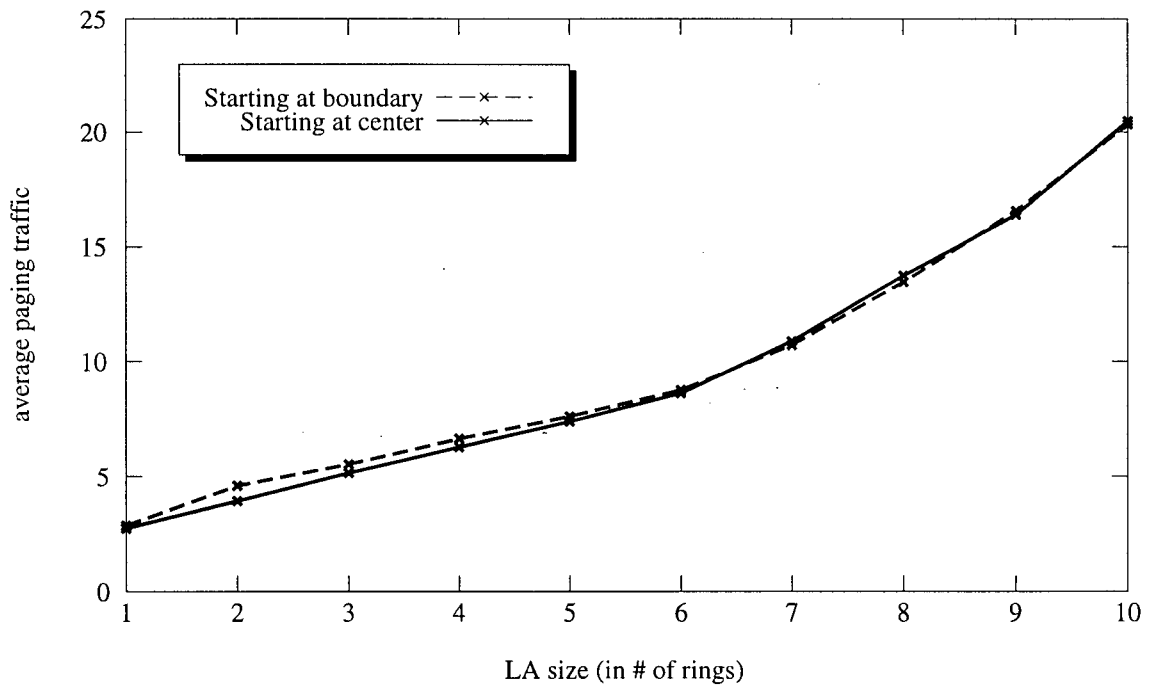
(b)

Figure 4.11 Performance of *Scheme A* when a different LA entry point is used with $\bar{v}$ = 40 km/hr, $\overline{t_h}$ = 60 sec, r_{cell} = 1 km, and λ_{call} = 1 call/hr. (a) average paging delay. (b) average paging traffic.

Chapter 5   SENSITIVITY OF PAGING SCHEMES TO UNCERTAINTY IN MOBILITY PARAMETER VALUES

In Chapter 4, three different paging schemes, *Selective paging, generalized paging with time-stamp (Scheme A)*, and *generalized paging without time-stamp (Scheme B)* were examined. For all three paging schemes, the system estimates the mobile user's position using the estimates of the user mobility parameters. These parameters include the mean speed ($\bar{v}$), mean velocity hold time ($\bar{t}_h$), and angular deviation parameter (α_θ). So far, we assumed that the system had the exact parameter values for the mobile user when evaluating the paging schemes' performance. However, we also need to consider the effects of uncertain mobility parameter values on the paging schemes' performance in terms of the average paging delay and traffic. In this chapter, the sensitivity of these three paging schemes to uncertainty in mobility parameter values are examined. Throughout this chapter, the destination is assumed to be at infinite distance. Also, the radius of a cell and call arrival rate are assumed to be 1 km and 1 call/hr, respectively. As in Section 4.8.1, the numbers of cells (N_c) in each paging group of LA sizes 1 through 10 are as follows: 3, 4, 5, 6, 7, 8, 10, 13, 16, and 20.

5.1 Uncertainty in Mean Speed

We let the system's mobility parameter estimates be $\bar{v} = 40$ km/hr, $\bar{t}_h = 60$ sec, and $\alpha_\theta = 4.2$ (95% criterion). The user has the same set of mobility parameters except for $\bar{v}$. We will consider two cases where the actual user's mean speeds are set to be 20 km/hr in case 1 and 60 km/hr in case 2. Then the performances of *Scheme A* and *Scheme B* are compared to that of
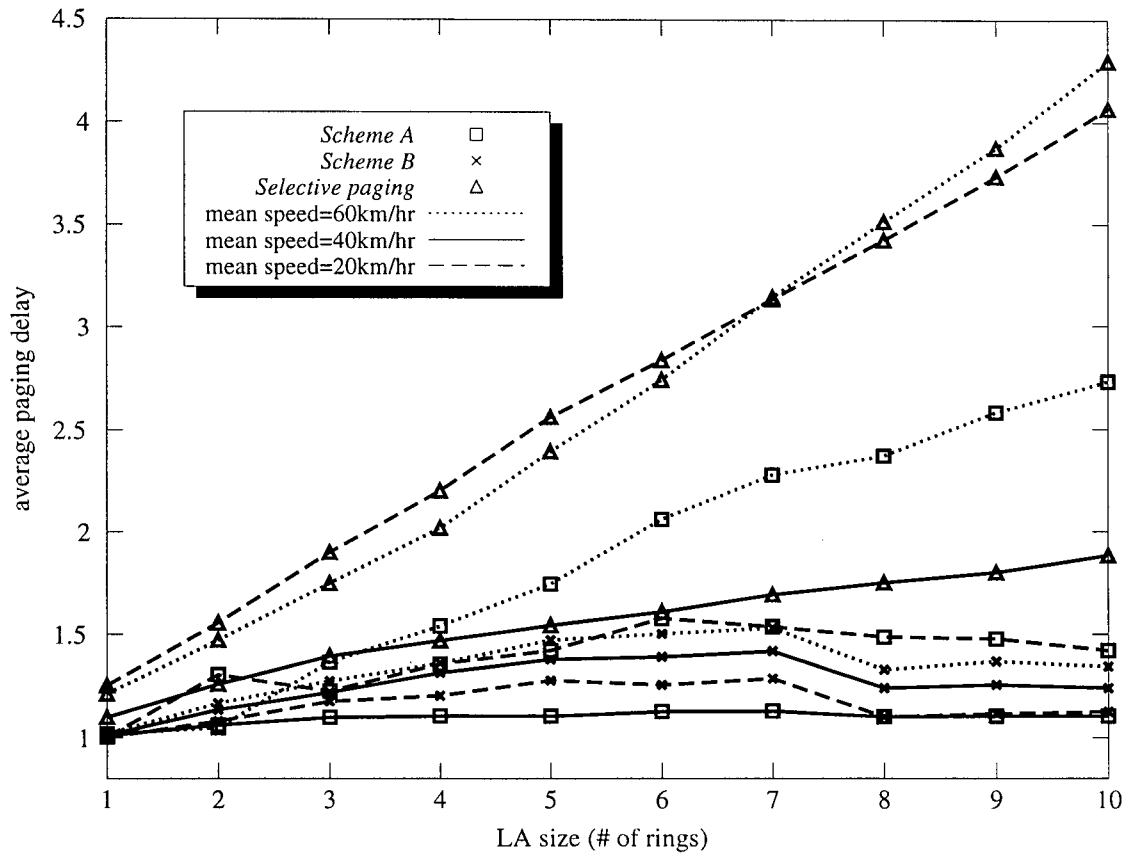
Figure 5.1   Sensitivity of the average paging delay performances of *Selective paging, Scheme A*, and *Scheme B* to uncertainty in $\bar{v}$ for $\bar{t}_h$ = 60 sec, $\bar{d}$ = ∞, α_θ = 4.2, r_{cell} = 1 km, λ_{cell} = 1 call/hr and the system's $\bar{v}$ = 40 km/hr.

Selective paging. Figure 5.1 and Figure 5.2 show the changes in average paging delay and traffic values. It is found that *Scheme B* is not very sensitive to the changes in the user's mean speed while *Scheme A* and *Selective paging* show significant increases in the average paging delays and traffics.

When the actual user's mean speed is 20 km/hr or 60km/hr and the system's mean speed estimate is 40 km/hr, *Scheme B* performs better than the other two schemes because it does not require the elapsed time since the last location update to make paging decisions. The system does not need to estimate the distance the user may have travelled since the last location update and
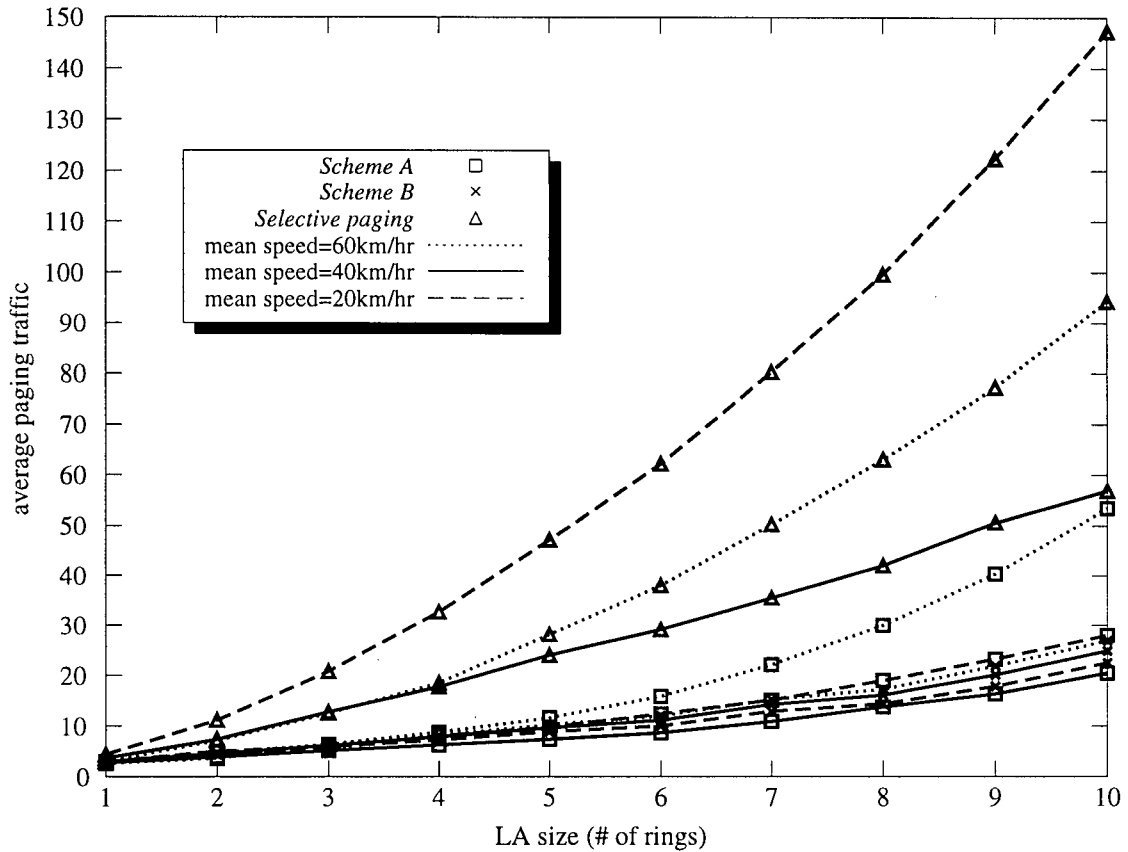
Figure 5.2   Sensitivity of the average paging traffic performances of *Selective paging*, *Scheme A*, and *Scheme B* to uncertainty in $\bar{v}$ for $\bar{t}_h$ = 60 sec, $\bar{d}$ = ∞, α_θ = 4.2, r_{cell} = 1 km, λ_{cell} = 1 call/hr and the system's $\bar{v}$ = 40 km/hr.

pages the same cells all the time. For *Scheme A* and *Selective paging*, the system underestimates or overestimates the distance the user may have travelled since the last location update and ends up paging cells with less probability of finding the user, resulting in increased average paging delay and traffic. However, the results show that *Scheme A* still performs better than *Selective paging*. In case 1 where the user's actual mean speed is 20 km/hr, *Scheme A*'s average paging delay increases from 1.04 to 1.42 and average paging traffic increases from 20.47 to 28.02 for an LA of size 10, but the *Selective paging*'s average paging delay increases from 1.89 to 4.06 and average paging traffic increases from 56.90 to 147.29. In the case 2 where the user's actual mean speed is 60 km/hr, *Scheme A's* average paging delay increases from 1.04 to 2.73 and average

paging traffic increases from 20.47 to 53.51 for an LA of size 10, whereas *Selective paging*'s average paging delay increases from 1.89 to 4.30 and average paging traffic increases from 56.90 to 94.39. In both cases, *Scheme A* results in lower average paging delays and traffics than *Selective paging*. It is also noted that *Scheme A*'s increase in the average paging traffic in case 2 is much greater than in case 1. This is because when the user's mean speed is higher, the cell probabilities become more spread out within an LA and the system requires to page more cells to find the user. For *Selective paging*, the average paging traffic in case 1 is much higher than in case 2 because the system overestimates the distance the user may have travelled since that last location update and tends to page the outer rings with more cells first.

5.2 Uncertainty in Mean Velocity Hold Time

We let the system's mobility parameter estimates be $\bar{v}$ = 40 km/hr, $\bar{t}_h$ = 60 sec, and α_θ = 4.2 (95% criterion). The user has the same set of mobility parameters except for $\bar{t}_h$. The user's actual mean velocity hold times are set to be 30 and 90 seconds. As shown in Figure 5.3 and Figure 5.4, all three schemes are not very sensitive to uncertainty in the mean velocity holding time. All changes in the average paging delays and traffics are within ±10% of the expected values. It is noted that the average paging delays and traffics increase slightly when the user's actual mean velocity hold time is greater than the system's estimate and decrease otherwise. When the user's mean velocity hold time is greater than the system's estimate, the user's angular deviation from the principal direction becomes larger and the system must page more cells in order to locate the user. When the user's mean velocity hold time is smaller than the system's estimate, the user's angular deviation from the principal direction becomes smaller and the system
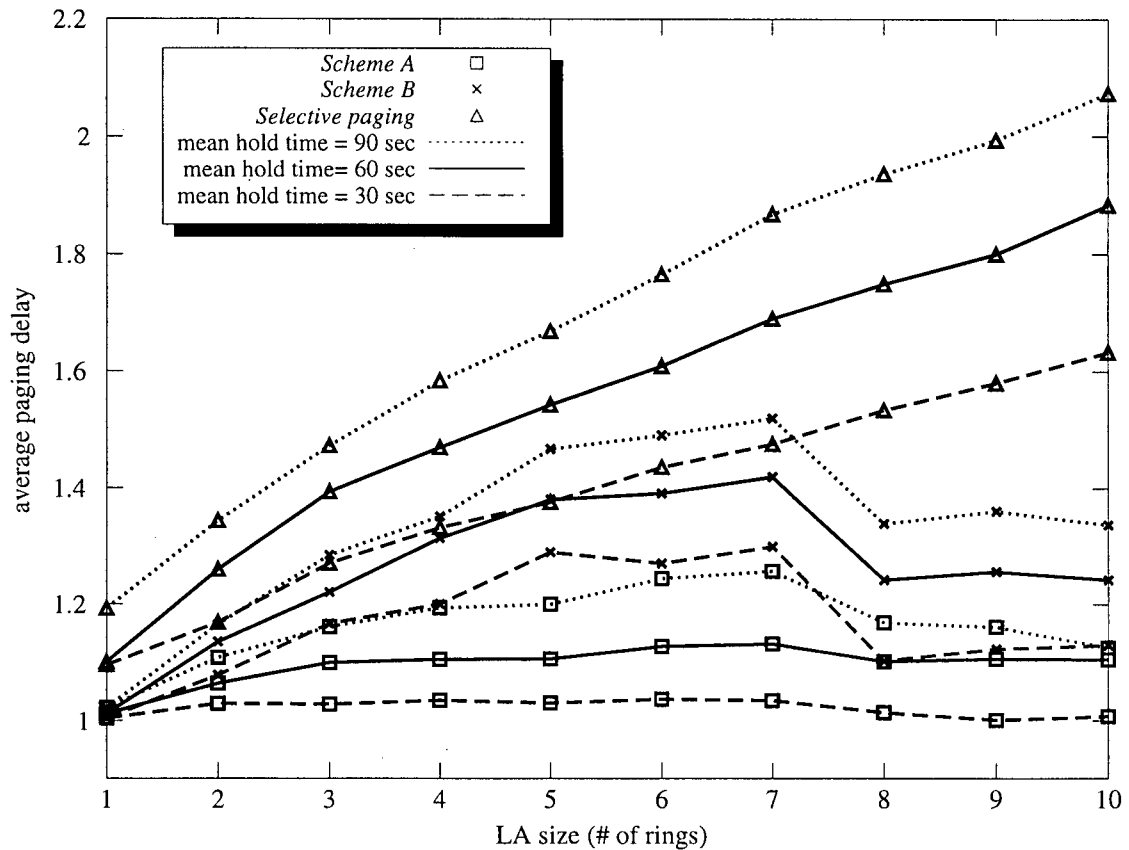
Figure 5.3   Sensitivity of the average paging delay performances of *Selective paging*, *Scheme A*, and *Scheme B* to uncertainty in $\bar{t}_h$ for $\bar{v}$ = 40 km/hr, $\bar{d}$ = ∞, α_θ = 4.2, r_{cell} = 1 km, λ_{cell} = 1 call/hr and the system's $\bar{t}_h$ = 60 sec.

can locate the user faster.

5.3 Uncertainty in Angular Deviation Parameter

The angular deviation parameter, α_θ, controls how much the user's angular direction deviates from the principal direction. In Section 2.1, we assumed that a mobile user moves in the forward direction with a probability of 0.95 (95% criterion) and the corresponding value of α_θ is 4.2. In this section, the user's actual angular deviation parameter value is changed to 1.4 (85% criterion) and 10.3 (98% criterion) to examine the three paging schemes' sensitivities on α_θ. We
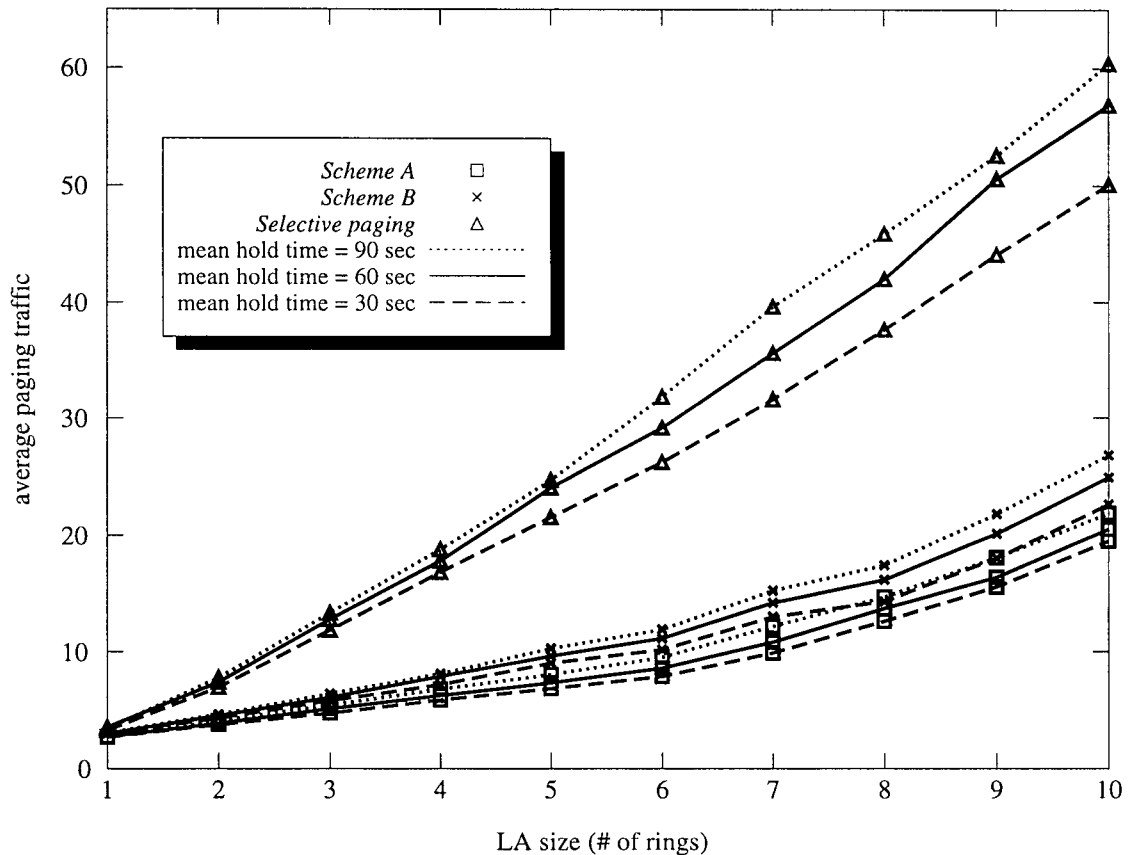
Figure 5.4   Sensitivity of the average paging traffic performances of *Selective paging*, *Scheme A*, and *Scheme B* to uncertainty in $\overline{t_h}$ for $\overline{v} = 40$ km/hr, $\overline{d} = \infty$, $\alpha_\theta = 4.2$, $r_{cell} = 1$ km, $\lambda_{cell} = 1$ call/hr and the system's $\overline{t_h} = 60$ sec.

let the system's mobility parameter estimates be $\overline{v} = 40$ km/hr, $\overline{t_h} = 60$ sec, and $\alpha_\theta = 4.2$. The user has the same set of mobility parameters except for α_θ.

Figure 5.5 and Figure 5.6 show the results. When the user's actual $\alpha_\theta = 10.3$, the average paging delay and traffic values do not change much for all three paging schemes. The performances of all three paging schemes improve slightly because the user's angular deviation from the principal direction becomes smaller and the probability of finding the user near the principal direction increases when α_θ increases. When the user's actual $\alpha_\theta = 1.4$, the three paging
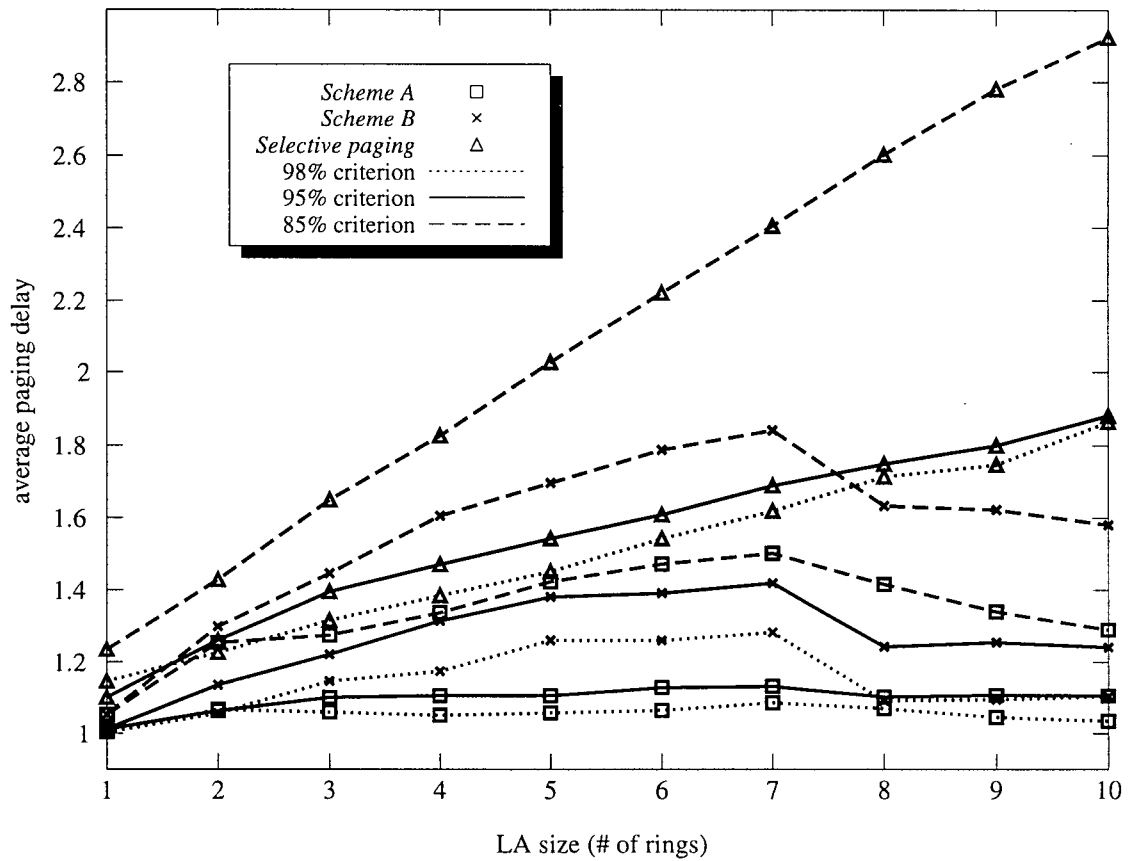
Figure 5.5   Sensitivity of the average paging delay performances of *Selective paging, Scheme A,* and
Scheme B to uncertainty in α_θ for $\bar{v}$ = 40 km/hr, $\bar{t}_h$ = 60 sec, $\bar{d}$ = ∞, r_{cell} = 1 km, λ_{cell} =
1 call/hr and the system's α_θ = 4.2.

schemes' average paging delay and traffic values all increase. However, the two *generalized paging* schemes still outperform *Selective paging*. For an LA of size 10, the average paging delay for *Selective paging scheme* increases from 1.89 to 2.92 while it increases from 1.04 to 1.29 and from 1.24 to 1.58 for *Scheme A* and *Scheme B,* respectively. Also, the average paging traffic for *Selective paging* increases from 56.90 to 100.54 while it only increases from 20.47 to 25.17 and from 24.84 to 31.62 for *Scheme A* and *Scheme B* respectively. *Scheme A* still results in the lowest average paging delay and traffic values.
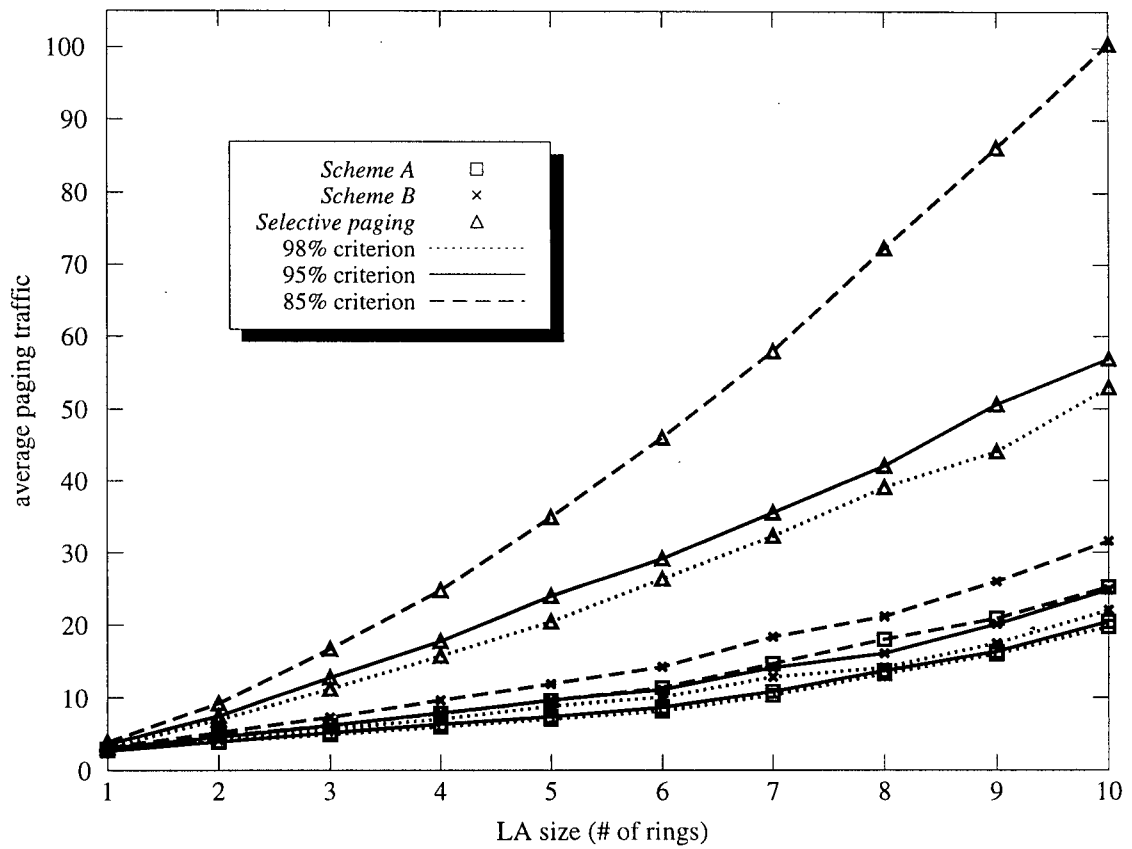
Figure 5.6   Sensitivity of the average paging traffic performances of *Selective paging*, *Scheme A*, and *Scheme B* to uncertainty in α_θ for $\bar{v} = 40$ km/hr, $\bar{t_h} = 60$ sec, $\bar{d} = \infty$, $r_{cell} = 1$ km, $\lambda_{cell} = 1$ call/hr and the system's $\alpha_\theta = 4.2$.

Chapter 6 MULTICASTING USING GENERALIZED PAGING SCHEMES

So far, the paging schemes have been only used to locate a single mobile user. However, there are some instances where more than one user needs to receive the same incoming call. For example, the system may need to page a taxi fleet for services. The system can page each user separately and deliver the call to one user at a time, but this method's average paging traffic is linearly proportional to the number of users. As an alternative, we can modify the two *generalized paging* schemes described in Chapter 4 to locate many mobile users within the service area in one paging process. In this chapter, *generalized multicasting* schemes are introduced to locate multiple users within the service area.

6.1 Preliminaries

The user's destination was assumed to be at infinite distance for the paging schemes in Chapter 4. Here we will assume that all mobile users move around within a service area of limited size. As before, each mobile user travels according to the mobility model described in Section 2.1 and its location is updated according to the location updating scheme described in Section 3.3. Each user's starting location and destination are uniformly distributed over the cells in the limited service area. Each user starts his journey from a randomly chosen source cell's center and travels toward a randomly chosen destination cell's center. As soon as he reaches the destination cell, he randomly chooses the next destination cell and starts the next journey from the center of the current cell. Although the user has not reached the center of the destination cell, the user is considered to be at the destination as long as he enters the destination cell. Figure 6.1 shows the possible movements of a mobile user within the service area.
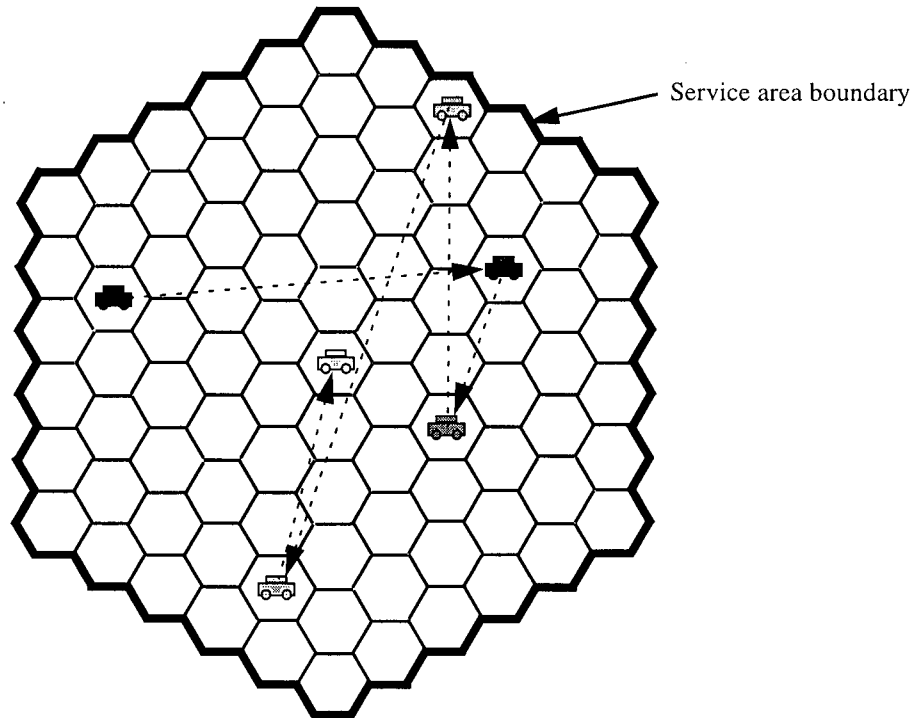
Figure 6.1 Mobile movements within the service area of size 5 (# of rings)

In [3], it is mentioned that each MSC handles about 100 cells. For the purpose of our analysis, the service area is assumed to have the size of 5 rings (= 91 cells) and each LA a size of 2 rings (= 19 cells).

6.2 Generalized Multicasting Schemes

For *generalized paging* schemes used to locate a single user, only the cell probabilities in one LA were considered in order to make paging decisions. In order to accommodate multiple users, we need to consider the cell probabilities in all mobile users' LA's at the same time. We first obtain the cell probabilities of the cells in each LA. If a cell belongs to more than one LA, its cell probabilities obtained from different LA's are added together. The resulting value, $P_{sum}(cell)$,for each cell represents the average number of mobile users residing in each cell. Note that the sum of
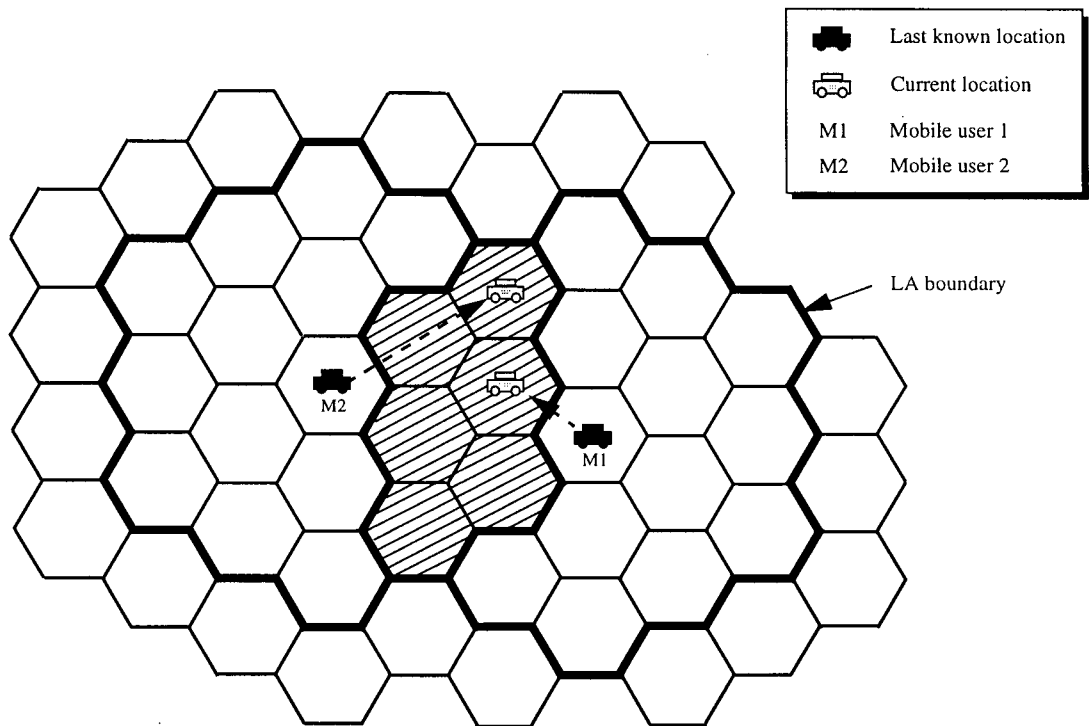
Figure 6.2 Overlapping of the two mobile users' LA's of size 2 (# of rings)

the LA cell probabilities for each user is 1. When we group the cells into a number of subsets,

$P_{sum}(cell)$'s obtained for all cells are divided by the number of mobile users in the service area

and are used as the new cell probabilities. The union of all LA's can be now considered as one big

LA with new cell probabilities.

A *generalized multicasting* scheme makes use of the fact that some LA's are bound to

overlap (partially or entirely) within the limited service area. Figure 6.2 shows an example of two

overlapping LA's. Because mobile user 1 and mobile user 2's LA's partially overlap each other,

and the two mobile users currently reside in the shaded overlapping area, we can expect to find

both of the users by paging these common cells first. As the number of mobile users in the service

area increases, more LA overlapping will occur and the *generalized multicasting* scheme's perfor-

mance, in terms of the average paging delay and traffic, is expected to improve.

Two different *generalized multicasting* schemes are presented. The first scheme, *generalized multicasting with time-stamp* (hereafter referred to as *Scheme C*), uses the location update time-stamp to estimate the mobile users' current locations as explained in Section 4.7.1. When a call comes in, the cell probabilities for each user are obtained based on each user's elapsed time, t_e, since his last location update as described in Section 4.8. The second scheme, *generalized multicasting without time-stamp* (hereafter referred to as *Scheme D*), uses static cell probabilities without using the location update time-stamp as explained in Section 4.7.2. The cell probabilities for each user are obtained as described in Section 4.8.

6.3 Simulation Results

The simulation results are presented in this section. The two *generalized multicasting* schemes' performances are measured in terms of their average paging delays and traffics. Figure 6.3 shows the relationships between the average paging delay and traffic values for the two schemes for the single user case. This figure differs from Figure 4.10 in two ways: (1) the LA size is 2. (2) the service area is limited to 5 rings.

The performances of the two schemes are shown in Figure 6.4. The average paging delay values for 10, 20, and 30 users are kept below the delay value for one user by using 34, 44, and 48 cells (N_C) for grouping each paging subset, respectively. Then, by looking at the average paging traffic values for different number of users, we can see that the performances of the two schemes improve significantly as the number of users in the service area increases. When the number of users increases from 1 to 30, the average paging traffic values only increase by a factor of 12 for
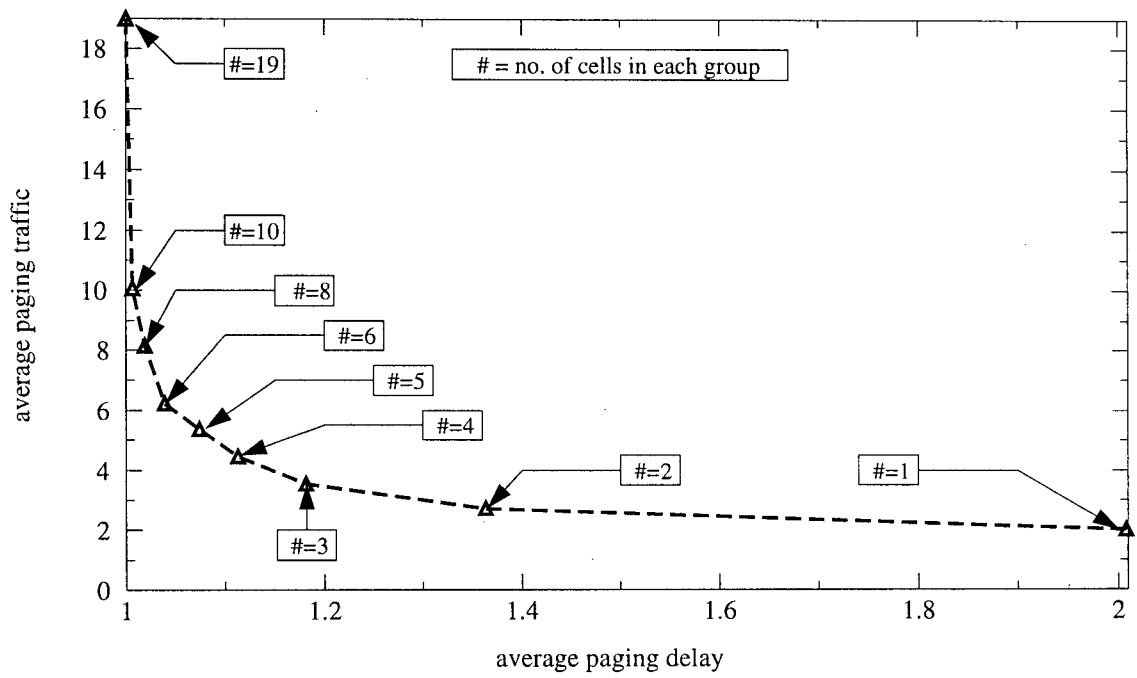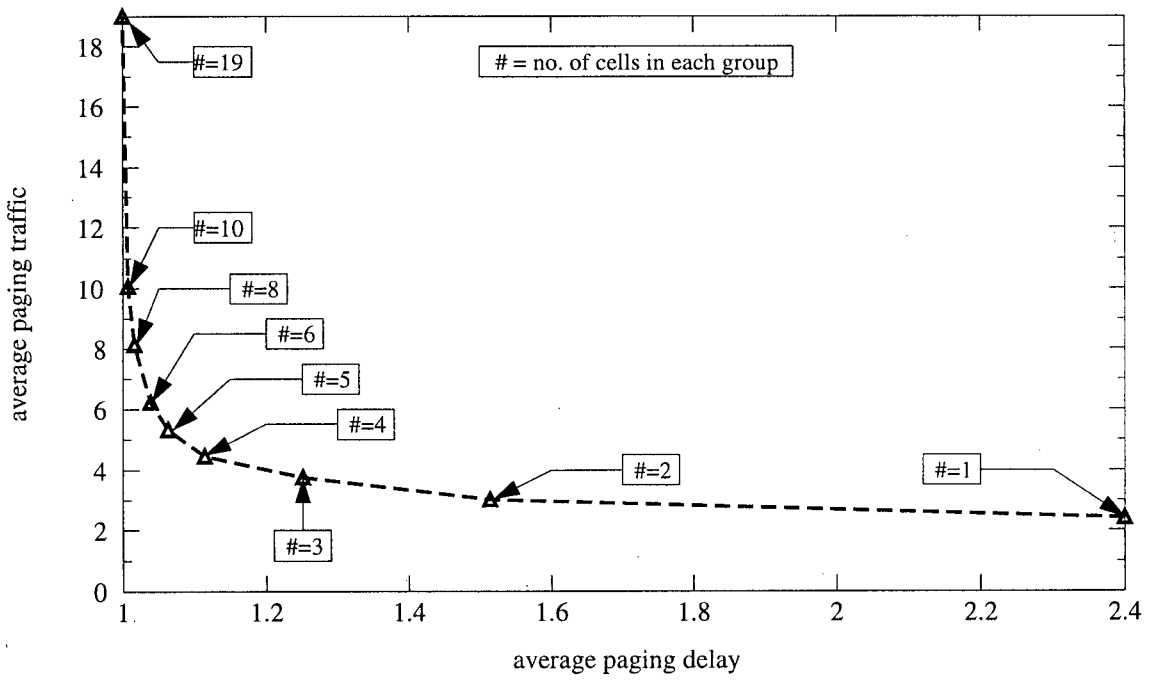
Figure 6.3 Average paging traffic versus average paging delay for single user with $\bar{v} = 40$ km/hr, $\overline{t_h} = 60$ sec, $r_{cell} = 1$ km, and $\lambda_{call} = 1$ call/hr, SA size = 5, LA size = 2, and # of users = 1. (a) *Scheme C.* (b) *Scheme D.*

both schemes.

We can see that the two schemes' average paging delay and traffic values are very close. This is due to the small service area and location area sizes chosen to reduce the time required for our simulations. Because there are not many cells in each LA, the two schemes' performances are very close to each other. The *Scheme C* is expected to outperform *Scheme D* by greater margins if larger service area and location area sizes are used.

(a)

(b)
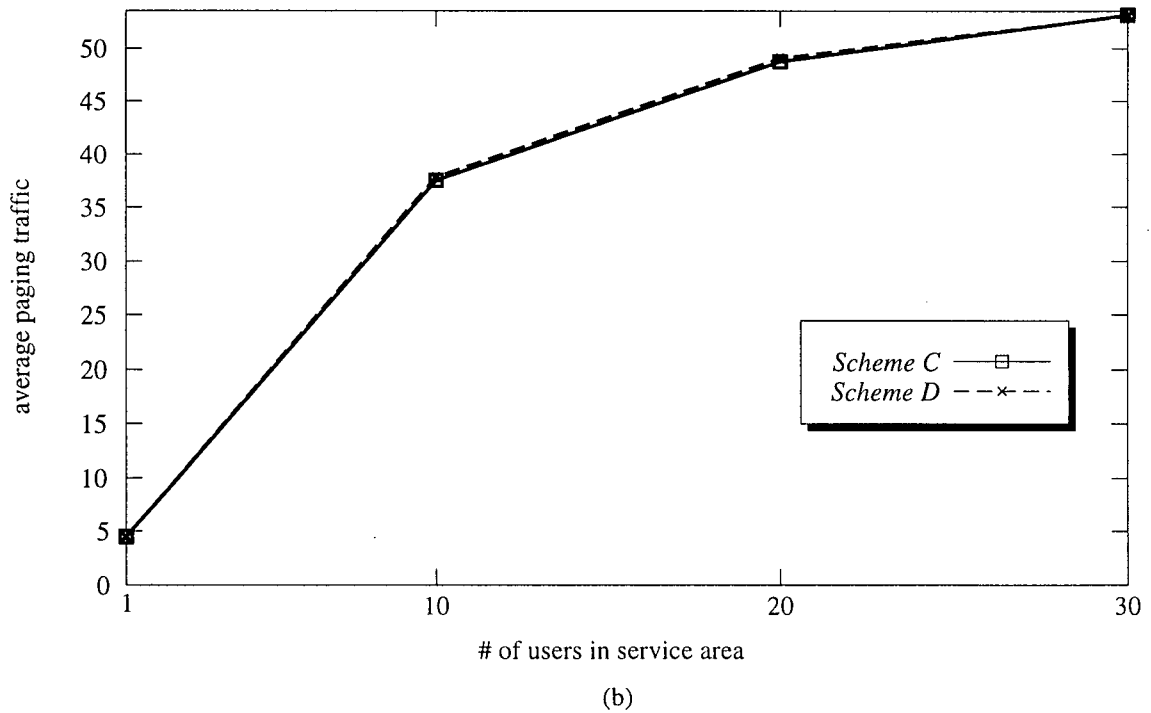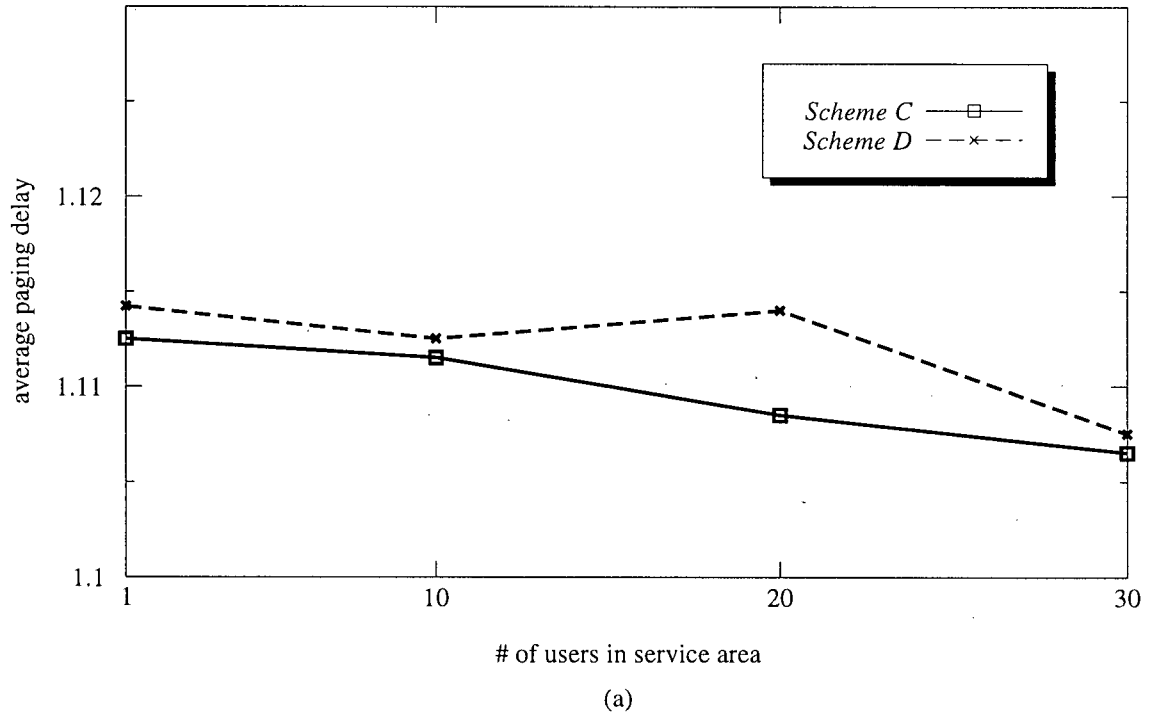
Figure 6.4 Performance of *Scheme C* and *Scheme D* with $\bar{v}$ = 40 km/hr, $\overline{t_h}$ = 60 sec, r_{cell} = 1 km, λ_{call} = 1 call/hr, SA size = 5, and LA size = 2. (a) average paging delay. (b) average paging traffic.

Chapter 7   CONCLUSION AND FUTURE WORK

This thesis has examined the problem of locating a mobile vehicular telephone user in a cellular system. Two LA paging schemes, called *generalized paging with time-stamp (Scheme A)* and *generalized paging without time-stamp (Scheme B)*, were proposed to determine the location of a user within an LA. For performance evaluation, a directional random walk model was used to model user mobility and a dynamic LA-based location updating scheme was used for user location registration. When compared to *Selective paging*, it was found that *Scheme A* and *Scheme B* can reduce both average paging delay and traffic considerably. For example, for an LA size of 10 and a subset size of 20, the average paging delay and traffic values are reduced by about 45% and 65% when *Scheme A* is used instead of *Selective paging* and by about 35% and 55% when *Scheme B* is used. Also, the *generalized paging* schemes can satisfy different performance needs (e.g. lower average paging delay and higher average paging traffic or vice versa) with different grouping parameters.

The sensitivity of the two generalized paging schemes to uncertainty in user mobility parameter values (i.e. mean speed, mean velocity hold time, and angular deviation parameter) was studied. *Scheme A* was found to be very sensitive to uncertainty in user mean speed whereas *Scheme B* was not very sensitive to changes in all three parameter values. For an LA size of 10, *Scheme A*'s average paging delay and traffic values increase by about 40% when the user's actual mean speed is 20 km/hr and the system's mean speed estimate is 40 km/hr; the corresponding increase for *Scheme B* is about -10%. When the user's actual mean speed is 60 km/hr and the system's mean speed estimate is 40 km/hr, *Scheme A*'s average paging delay and traffic values increase by about 160%; the corresponding increase for *Scheme B* is about 10%.

Two multicasting schemes, *generalized multicasting with time-stamp* (*Scheme C*) and *generalized multicasting without time-stamp* (*Scheme D*), were implemented using *generalized paging* schemes. As the number of users within a limited service area is increased, the performances of *Scheme C* and *Scheme D* improve significantly. When the number of users increases from 1 to 30, the average paging traffic values only increase by a factor of 12 for both schemes while the average paging delay values are kept below the delay value for one user.

Among the topics which could be further investigated are:

- To analyze paging scheme performances using different mobility models.

- To analyze paging scheme performances using different location updating schemes (e.g. time-based, movement-based, or distance-based scheme [1]).

- To analyze the effects of using different criteria (other than the average number of users in a cell) for selecting cells to be paged in multicasting.

Bibliography

[1] I. F. Akyildiz and J. Ho, "On Location Management for Personal Communications Networks", *IEEE Commun. Mag., pp.* 138-145, Sep. 1996.

[2] T. S. Rappaport, "The Wireless Revolution", *IEEE Commun. Mag., pp.* 52-71, Nov. 1991.

[3] S. Madhavapeddy and K. Basu, "Optimal Paging in Cellular Mobile Telephone Systems", *Proc. of the 14th International Teletraffic Congress, ITC 14, Antibes, France, pp.* 493-502, June 1994.

[4] H. Jung, S. Mishra, and O. K. Tonguz, "Efficient Location Management in PCS", *Proc. of the 6th International Symposium on Personal, Indoor and Mobile Radio Communications, pp.* 284-288, 1995.

[5] S. Okasaka, S. Onoe, S. Yasuda, and A. Maebara, "A New Location Updting Method for Digital Cellular Systems", *Proc. of the 41st IEEE Vehicular Technology Conference, pp.* 345-350, 1991.

[6] H. Xie, S. Tabbanc, and D. J. Goodman, "Dynamic Location Area Management and Performance Analysis", *Proc. IEEE VTC'93, pp.* 536-539, May 1993.

[7] S. Madhavapeddy, K. Basu, and A. Roberts, "Adaptive Paging Algorithms for Cellular Systems", *Fifth WINLAB Workshop on Third Generation Wireless Information Networks,* New Brunswick, NJ, *pp.* 976-980, April 1995.

[8] D. Munoz-Rodriguez, "Cluster Paging for Traveling Subscribers", *Proc. of the 40th Vehicular Technology Conference, pp.* 748-753, May 1990.

[9] A. Yener and C. Rose, "Paging Strategies for Highly Mobile Users", *Proc. of the 46th IEEE Vehicular Technology Conference, pp.* 1839-1842, 1996.

[10] M. Shirota, Y. Yoshida, and F. Kubota, "Statistical Paging Area Selection Scheme for Cellular Mobile Communication Systems", *Proc. the 44th IEEE Vehicular Technology Conference, pp.* 367-370, 1994.

[11] K. Lam, *Location Updating and Paging Strategies in a Cellular System*, M.A.Sc. thesis, Department of Electrical Engineering, University of British Columbia, 1993

[12] I. F. Akyildiz, J. Ho, and Y. Lin, "Movement-Based Location Update and Selective Paging for PCS Networks", *IEEE/ACM Transactions on Networking, Vol. 4, No. 4, pp.* 629-638, Aug. 1996.

[13] A. Nakajima, M. Eguchi, T. Arita and H. Takeda, "Intelligent Digital Mobile Communications Network Architecture," *Proc. of XIII International Switching Symposium, Stockholm, Sweden, vol. VI,* May-June 1990.

[14] W. C-Y. Lee, *Mobile Cellular Telecommunication Systems,* McGraw Hill, 1989.

[15] W. W. Erdman, "Wireless Communications: A Decade of Progress", *IEEE Commun. Mag., pp. 48-51,* Dec. 1993.

[16] J. Markoulidakis, G. Lyberopoulos, D. Tsirkas, and E. Sykas, "Mobility Modeling in Third-Generation Mobilie Telecommunications Systems", *IEEE Personal Communications, Vol 4, Issue 4, pp.* 41-56, Aug. 1997.

[17] H. Xie and D. Goodman, "Mobility Models and Biased Sampling Problem", *Proc. of 2nd IEEE International Conference on Universal Personal Communications,* Ottawa, 1993.

[18] P. Camarda, G. Schiraldi, F. Talucci, and R. Valla, "Cellular Communication Mobility Model for a Finite Multiclass Population of Users", *IEEE 47th Vehicular Technology Conference,* 1997.

[19] I. Rubin and C. W. Choi, "Impact of the Location Area Structure on the Performance of Signalling Channels in Wireless Cellular Networks", *IEEE Commun. Mag., pp.* 108-115, Feb. 1997.

[20] A. R. Potter, "Implementation of PCNs Using DCS1800", *IEEE Commun. Mag., pp.* 32-36, Dec. 1992.

[21] T. Sakamoto, E. Kamagata, and M. Serizawa, "Location Registration and Paging for In-building Personal Multi-media Communication Systems",

[22] Y. Lin, "Modeling Techniques for Large-Scale PCS Networks", *IEEE Commun. Mag., pp.* 102-107, Feb. 1997.

[23] C. Rose and R. Yates, "Location Uncertainty in Mobile Networks: A Theoretical Framework", *IEEE Commun. Mag., pp.* 94-101, Feb. 1997.

[24]   N. Kennedy, *Fundamentals of Traffic Engineering, 8th edition*, Berkeley, Calif. Inst. of Traffic and Transportation Engineering, Univ. of Calif. Berkeley, 1973.

[25]   D. L. GerLough and M. J. Huber, *Traffic Flow Theory*, Transportation Research Board, National Research Council, Washinton, D. C., 1975.

[26]   H. J. W. Leong, "The distribution and Trend of Free Speeds on Two-Lane Rural Highways in New South Wales," *Proc. Austr. Road Res. Board, 4: pp.* 791-814, 1968.